Is the Permian–Triassic Mass Extinction Related to the Siberian Traps?

Krivolutskaya, N. A.; Konyshev, A. A.; Kuzmin, D. V.; Nikogosian, I. K.; Krasheninnikov, S. P.; Gongalsky, B. I.; Demidova, S. I.; Mironov, N. L.; Svirskaya, N. M.; Fedulov, V. S.

published in
Geochemistry International
2022

DOI (link to publisher)
10.1134/S0016702922130067

document version
Publisher's PDF, also known as Version of record

ISSN 0016-7029, Geochemistry International, 2022, Vol. 60, No. 13, pp. 1323–1351. © Pleiades Publishing, Ltd., 2022.

Is the Permian–Triassic Mass Extinction Related to the Siberian Traps?

N. A. Krivolutskaya[a, *], A. A. Konyshev[b], D. V. Kuzmin[c], I. K. Nikogosian[d], S. P. Krasheninnikov[a], B. I. Gongalsky[e], S. I. Demidova[a], N. L. Mironov[a], N. M. Svirskaya[a], and V. S. Fedulov[a]

[a] *Vernadsky Institute of Geochemistry and Analytical Chemistry, Russian Academy of Sciences, Moscow, Russia*

[b] *Institute of Geology of Karelian Research Centre, the Russian Academy of Sciences, Petrozavodsk, Russia*

[c] *V.S. Sobolev Institute of Geology and Mineralogy, Siberian Branch of the Russian Academy of Sciences, Novosibirsk, Russia*

[d] *Faculty of Science, Vrije Universiteit, Amsterdam, The Netherlands*

[e] *Institute of Geology of Ore Deposits, Petrography, Mineralogy, and Geochemistry of Russian Academy of Sciences, Moscow, Russia*

**e-mail: nakriv@mail.ru*

Received June 17, 2022; revised August 31, 2022; accepted September 2, 2022

Abstract—The Siberian Traps are believed to play an essential role in the Permian–Triassic extinction event, although the link between these events is unclear. Plume ascent, its interaction with the lithosphere, and crustal rocks are considered as sources of volatile components that trigger mass extinction. Reliable estimations of the volumes of gases released during the basalt magma degassing that formed typical traps are few. In this work, the volatile contents in the parental melt of the Southern Maslovsky intrusion, which is a part of the PGE–Cu–Ni Maslovsky deposit in the Norilsk district in the Northwest Siberian Platform, were determined. The studied intrusion belongs to the ore-bearing Norilsk intrusive complex, which is coeval to the Morongovsky–Mokulaevsky Formations of the Siberian flood basalt province. The objects of this study were 8 silicate-melt inclusions in olivines from picritic gabbro-dolerites and 68 inclusions in clinopyroxenes, and 2 inclusions in olivines from olivine-bearing gabbro-dolerites. The composition of the parental melt in terms of major and trace element abundances was close to the main stage of the platform magmatism. The average volatile contents in melt inclusions were as follows: 4500 ppm H_2O and Cl 1333 ppm, followed by trace amounts of F 387 ppm, S 743 ppm, CO_2 1279 ppm, and B 4.18 ppm, typical of within-plate magmas. In addition, the contacts of igneous rocks with sedimentary deposits (carbonate-terrigenous rocks and coals) demonstrate the occurrence of narrow zones of alteration and the absence of a significant volume of gases that could influence the process of species extinction. There is no strict evidence of the influence of the Siberian traps on the Permian–Triassic mass extinction.

Keywords: Siberian traps, PGE-Cu-Ni Maslovsky deposit, clinopyroxene, olivine, melt inclusions, volatiles, P-T mass extinction

DOI: 10.1134/S0016702922130067

INTRODUCTION

The Siberian magmatic province occupies a special place among the large igneous provinces due to (1) the large volume of magmatic rocks (Zolotukhin et al., 1975, 1986; Sharma, 1997; Al'mukhamedov et al., 2004; Elkins-Tanton, 2005; Ernst, 2014; Vinnik et al., 2017), (2) the occurrence of unique platinum–copper-nickel deposits in its northwestern part (Godlevsky, 1959; Dyuzhikov et al., 1992; Naldrett, 2004; Likhachev, 2006; Krivolutskaya, 2016; Radko, 2016), and (3) the proximity of the time of its formation to the most significant mass extinction of species in the history of Earth at the Permian–Triassic (P–T) boundary (Renne and Basu, 1991; Campbell et al., 1992; Kamo et al., 2003; Reichow et al., 2009; Sobolev et al., 2011; Elkins-Tanton et al., 2020, 2021). All these three features could be primarily related to each other and require genetic interpretation. Studies based on them have gathered significant attention to the Siberian province over the past few decades (Ernst, 2014; Elkins-Tanton et al., 2020; Lightfoot et al., 1990, 1993; Wooden et al., 1993; Ryabchikov et al., 2001, 2001a; Sibik et al., 2015, 2021; Davydov and Karasev, 2021; Davydov et al., 2021).

Terminology. The formation mechanisms of the Siberian magmatic province and associated deposits significantly depend on the concepts that are embedded in the names of areas of volcanic rocks. Recently, the term "Siberian traps province" has been used for all Siberian magmatic rocks close in age (251 Ma, (Kamo et al., 2003)), including Kuzbass, Altai, and Ural, without considering their geological features (Reichow

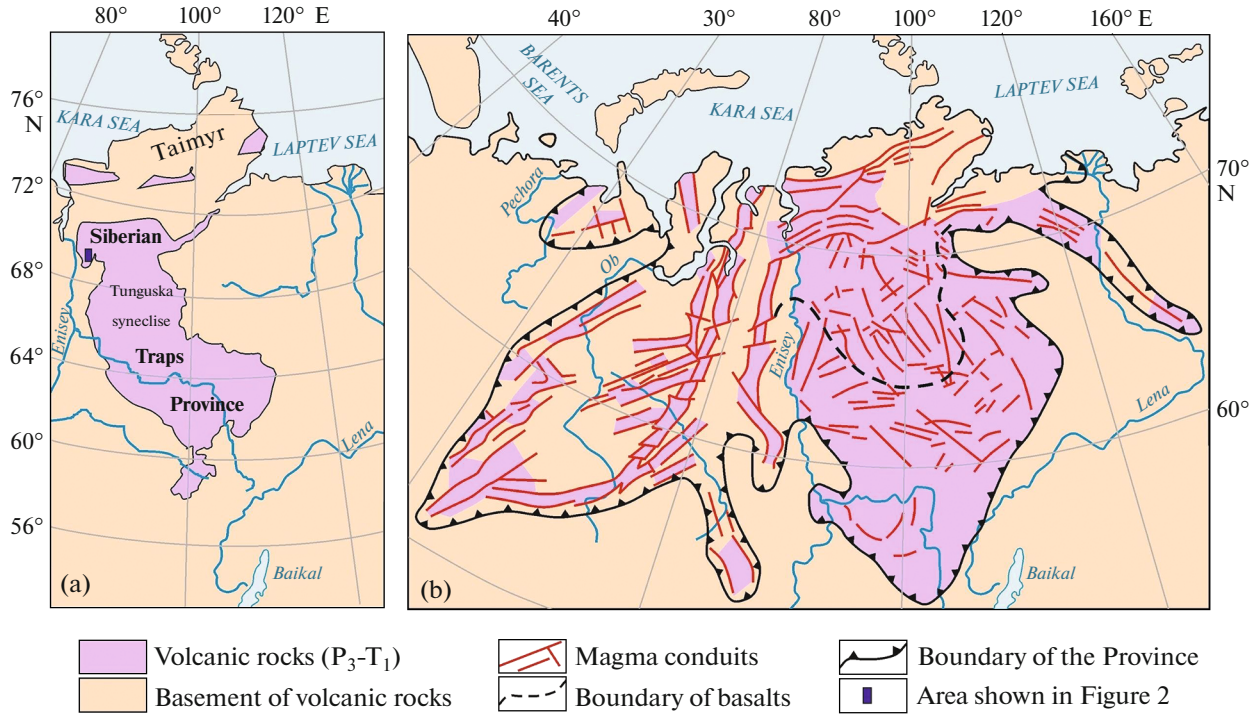

Fig. 1. Schematic maps of the Siberian Traps Province (a) and Siberian large Igneous Province (b) (boundaries of the provinces after: a—Zolotukhin et al., 1986; b—Masaitis, 1983).

et al., 2009; Saunders and Reichow, 2009; Svetlitskaya and Nevolko, 2016). However, all these rocks cannot be attributed to traps because the concept of traps presupposes (1) the geological structure of the flows (covers), (2) tectonic position, and (3) chemical composition. Hence, traps are basalts with sustained thickness, covering huge areas on ancient platforms (flood basalts) and having a mostly tholeiitic composition (Geological Dictionary, 2009; Staroseltsev, 1989; Krivolutskaya and Kedrovskaya, 2020). The characteristics of the Siberian traps (Tuklonsky, Morongovsky–Samoedsky Formations in the Norilsk area and their analogs: the Ayansky–Khonnamakitsky and Kochechumsky–Nidymsky Formations in the Putorana plateau and Tunguska syneclise, respectively) are as follows: 6–7 wt % MgO (120 analyses; Zolotukhin et al., 1986; Urvantsev, 1974), 1.48–1.58 Gd/Yb, and 2.14–2.81 La/Sm (48 analyses; Krivolutskaya and Kedrovskaya, 2020), $^{87}Sr/^{86}Sri$ = 0.70466–70653, ε_{Nd} = 0.14–1.90; $^{206}Pb/^{204}Pb$ = 18.231–18.844 (31 analyses, Lightfoot et al., 1993; Wooden et al., 1993). The Siberian Traps, Deccan Traps, Parana–Etendeka Traps, and Columbia River Basalt Group are a few continental trap provinces on Earth. Figure 1a illustrates the boundaries of the Siberian Traps province. The Siberian Platform and the southern part of the Taimyr Peninsula forming the Siberian Craton are covered by traps (Urvantsev, 1974; Geological Map..., 2005). The other volcanic rocks close to the traps in the time of formation are confined exclusively to extended rift zones (Fig. 1b). First, they were combined with typical traps by Masaitis (1983) (Fig. 1b). The rifting basalts form small, rapidly pinching out flows that do not have a large area of distribution and are confined to linear structures (paleorift zones); their composition varies significantly from subalkaline and alkaline rocks to ultrabasic rocks in Eastern Siberia (Syradasaysky, Ivakinsky–Nadezhdinsky, and Arydzhangsky–Maymechinsky Formations) and acidic rocks in Western Siberia: MgO = 3–5 to 22–24 wt % (Zolotukhin et al., 1986; Urvantsev, 1974), La/Sm = 2.4–5.72, and Gd/Yb = 1.6–7.9, $^{87}Sr/^{86}Sr_i$ = 0.70302–0.71114, ε_{Nd} = −11.0 to +6.6, $^{206}Pb/^{204}Pb$ = 17.796–19.111 (Wooden et al., 1993; Arndt et al., 1995, 2003; Vasil'ev et al., 2017). As a rule, small volcanoes of central type are often present in these zones.

These fundamental differences between two types of magmatism (Zolotukhin et al., 1989; Wooden et al., 1993; Al'mukhamedov et al., 2004)—rift and platform (or traps *per se*)—are crucial both for the formation mechanisms of large igneous provinces (LIPs) and for conditions of magmatic sulfide deposits. Therefore, considering the volcanism of Siberia and associated intrusive complexes, terminologically different formations should be distinguished using the Siberian traps province or Siberian flood basalts province (SFBP) and the Siberian large igneous province (SLIP). The latter can be subdivided into Western Siberian large igneous provinces and Eastern Siberian large igneous provinces (with SFBP as the main part). For each type

of volcanism, it is necessary to make separate stratigraphic columns and not combine them, which leads to incorrect conclusions about the volcanic thickness. For instance, summarized basalt thickness was estimated to be 6.5 km due to the combination of two different sections (Fedorenko and Czamanske, 1997; Kamo et al., 2003), while magmatism occurred consistently in different places and did not exceed 3.5 km.

These differences between the two types of basalts should also be included when considering the role of the SLIP in the *P–T* boundary biotic crisis because data on rift rocks with a very local distribution are often extended to the whole province. However, the contribution of basalts to mass extinction is mainly based on the data on Eastern Siberia because of (1) its several times greater volume of igneous rocks than Western Siberia and (2) its well-exposed and well-studied igneous rocks, unlike those in Western Siberia described only in boreholes. The results of our work are also related to Eastern Siberia and are considered an example of typical trap rocks (SFBP), i.e., syngenetic intrusive rocks.

The problems. The volatile components in magmas (H_2O, CO_2, Cl, and F) are of great importance to the studies of the origin of magmatic deposits, such as the unique PGE–Cu–Ni Norilsk deposits, the formation mechanisms of the Siberian traps, and mass extinction.

First, the selective gabbro intrusions in the Norilsk region of economic potential have led to studies about ore formation. One suggested the enrichment of ore-bearing magmas in volatile components compared with the other massifs (Distler et al., 1999). Despite widespread this idea (Barnes et al., 2019; Yao and Mungall, 2020), magma's volatile contents have not been directly determined. Second, the genesis of the magmas that formed the Siberian Traps province has been a topic of discussion over the past few decades, including their formation in the subduction processes (Ivanov, 2007). This hypothesis requires, in particular, a comparison of the fluid regime of trap magmas with the magmas formed at other tectonic regimes.

Finally, the link between the timing of trap formation and the *P–T* life extinction (Campbell et al., 1992) was established, leading to the assumption of volcanism as the main reason for mass extinction (90% of marine species and 75% of terrestrial species) on Earth at the *P–T* boundary. Other ideas about the causes of life extinction, including the natural evolution of life and shock events, have been put forward, but the volcanic contribution to life extinction is the most popular. The extinction mechanisms have also been actively discussed when this event is analyzed. Most researchers have considered a change in volatile components (CO_2 and other gases) in the atmosphere as the main factor of the biotic crisis (Sobolev et al., 2015; Black et al., 2014). There are two sources of volatiles, according to an opinion (Black et al., 2012, 2014): (1) basaltic magmas forming SFBP and (2) sedimentary rocks that underwent intruded magmatic heating (mostly carbonate rocks and coals).

Thus, determining H_2O, Cl, S, and CO_2 contents in basalts is very important. The volatile contents have been measured in melt inclusions in many rocks of the SLIP, but almost all of them characterize rift magmatism, i.e., Maymechinsky, Gudchikhinsky, and Arydzhangsky Formations (Ryabchikov et al., 2001, 2001a, 2009; Vasil'ev et al., 2017; Sobolev et al., 2009, 2009a). On the other hand, data on SFBP are limited (Krivolutskaya and Sobolev, 2001; Black et al., 2012, 2014; Sibik et al., 2015). In addition, the last rocks are the most important for solving the mentioned problems.

In this work, we decided to reduce this gap by tracing both possible sources of volatiles. First, we measured them in melt inclusions in the ore-bearing Maslovsky intrusion, and second, we regarded the interaction of magmas with the surrounding rocks to estimate their contribution to the balance of volatiles.

BRIEF INFORMATION ABOUT THE GEOLOGICAL STRUCTURE OF THE EAST SLIP

The volcanic rocks (SFB) are widespread on the Siberian Platform and the southern Taimyr (Fig. 1a), covering a large Siberian Craton, the crystalline basement of which is overlapped by a powerful cover of sedimentary rocks (from Riphaean to Middle Permian; (Dyuzhikov et al., 1992)). The maximum thickness of deposits reaches 12 km in the Tunguska syneclise. They are represented by marine carbonate-terrigenous sulfate-bearing rocks ($V–C_1$) in the lower part of the sequence and by continental coal-bearing deposits ($C_2–P_2$), combined into the Tunguska series in its upper part (Figs. 2a, 2b). A thick tuff-lavas pile ($P_3–T_1$) covers the sedimentary deposits. Its maximum thickness occurs north of the Siberian Platform in the Norilsk and Maymecha-Kotuy areas (up to 3.5 km) due to the combination of rift and platform basalts in one section. Eleven formations were recognized in the Norilsk (from bottom to top): Ivakinsky, Syverminsky, Gudchikhinsky, Khakanchansky, Tuklonsky, Nadezhdinsky, Morongovsky, Mokulaevsky, Kharaelakhsky, Kumginsky, and Samoedsky (Dyuzhikov et al., 1992). Trap rocks begin from the Tuklonsky Formation and have great importance for assessing the content of volatile components in magmas.

Intrusive rocks related to flood basalts are represented by gabbro-dolerite sills, similar in composition to typical traps (6–7 wt % MgO) localized mainly in sediments of the Tunguska series, rarely in the Silurian-Devonian rocks. They intruded in Early Triassic time. The thickness of sills varies significantly from a few meters to 400–450 m. They belong to the Katangsky complex (*Geological Map*..., 2005).

The Norilsk intrusive complex has distinctly differentiated intrusions of increased magnesium content

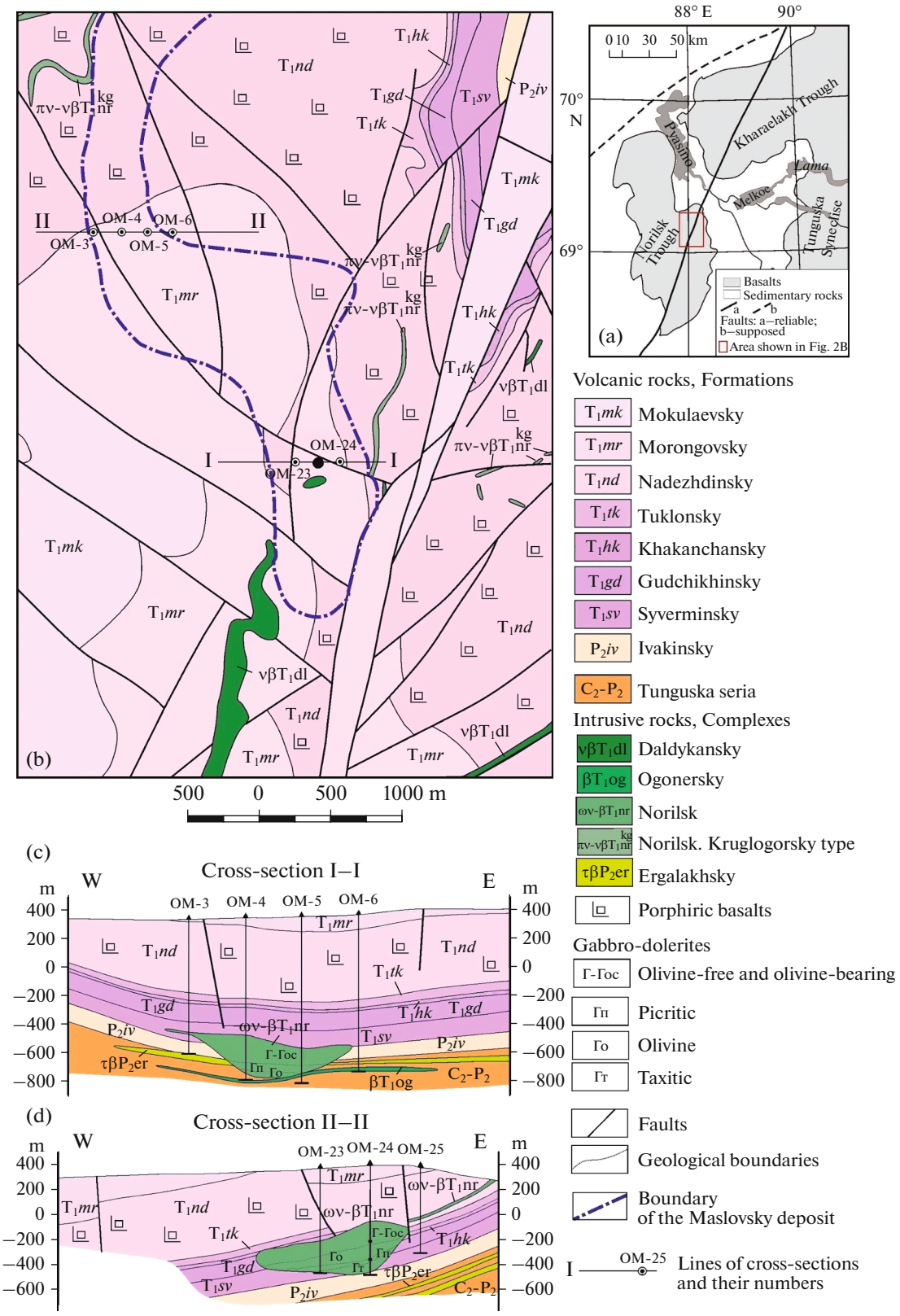

Fig. 2. Setting of the Maslovsky deposit in the Norilsk area (a) and geological map (b) and cross-sections (c, d) of the Maslovsky deposit (after the Ltd. Norilskgeology data).

(10–12 wt % MgO) and contains sulfide mineralization. They are concentrated northwest of the Siberian Platform (Fig. 1a). They are ribbon-shaped bodies with a length of up to 20 km, a width of 2–3 km, and a thickness of 150 m (the Talnakh, Norilsk 1, and Pyasino–Vologochansky intrusions) (Dyuzhikov et al., 1992; Proceedings of the Sudbury-Noril'sk symposium, 1994).

As a rule, they lie in the Devonian rocks or the Tunguska series. Some intrusions form dyke-like bodies (Norilsk 2 and Bol'shaya Bariernaya). Subalkaline and alkaline rocks occur northeast of the Siberian Platform in the Maymecha-Kotuy district.

OBJECTS AND METHODS

Objects

To assess the fluid regime of traps magmatism, we studied the magmatic (melt and fluid) inclusions in the main rock-forming minerals of ore-bearing intrusions of the Norilsk complex, whose compositions and age are close to flood basalts, i.e., to the Morongovsky and Mokulaevsky Formations (Fedorenko et al., 1996; Krivolutskaya et al., 2001; Latyshev et al., 2020). These rocks have similar patterns of rare elements and isotopic characteristics (Lightfoot et al., 1990; Wooden et al., 1993; Nesterenko and Al'mukhamedov, 1973). We chose intrusive rocks to study melt inclusions because they provide more reliable information on volatile components than effusive rocks, which may undergo significant volatile degassing of the parental magma. The Maslovsky deposit (Figs. 2a–2d) is a very important object because it comprises rocks with large melt inclusions in rock-forming minerals. We investigated magmatic inclusions in olivines from the picritic gabbro-dolerites and in clinopyroxenes from olivine-bearing gabbro-dolerites that form its upper part (Fig. 2d).

The interaction of basalt magma with the host coal-bearing rocks of the Tunguska series was studied in the contact zone of the Talnakh intrusion (borehole SF-10) and the Kayerkan open pit in the Norilsk district. We studied contacts of the Katangsky sills with Ordovician and Devonian carbonate rocks in the Podkamennaya Tunguska (near Baikit village) and Kulyumber river valleys.

Methods

Experimental work. Single inclusions in pyroxenes and olivines were heated in a Sobolev–Slutsky heating stage (Sobolev and Slutsky, 1984; Sobolev et al., 2015) to determine their temperature of homogenization, while many inclusions were heated in a high-temperature furnace (Kargaltsev et al., 2009; at $T = 1190$°C for clinopyroxenes and $T = 1250$°C for olivines) with controlled oxygen fugacity (QFM) at the Vernadsky Institute of Geochemistry and Analytical Chemistry of Russian Academy of Sciences, Moscow (GEOKHI RAS; analysts A.A. Kargaltsev, S.P. Krasheninnikov).

The exposure time for melt inclusions in clinopyroxenes was 5 min to avoid loss of volatile components. As new phases in olivine-hosted melt inclusions grow during olivine heating (Krivolutskaya et al., 2001), the exposure time was increased at the homogenization temperature. This approach did not allow the determination of the water content in inclusions (Supplementary Table S1), but Cl and S have been measured. In both cases, the experimentally obtained glasses were quenched, mounted into checkers, and polished, and their compositions were analyzed. The minimum size of analyzed inclusions was 20 μm (4 inclusions), while the others (64 inclusions) were 30–70 μm. Thus, the representativeness of the melt inclusion compositions obtained by secondary ion mass spectrometry (SIMS, probe diameter 20 μm) and electron microprobe analyzer (EPMA) is beyond doubt.

Analytical work. Analysis of major elements in melt inclusions and rock-forming minerals was carried out using a Cameca SX-100 at GEOKHI RAS (analyst N.N. Kononkova), JEOL JXA 8200 at the Institute of Chemistry, Mainz, Germany (analysts D.V. Kuzmin, N.A. Krivolutskaya), and Tescan MIRA 3 field emission gun scanning electron microscope (GEOKHI RAS; analyst S.I. Demidova), which was equipped with an Oxford Instruments Energy-dispersive detector (EDS). The glass inclusions and surrounding minerals were analyzed with an accelerating voltage of 20 kV at a 15 mm working distance. Preliminary backscattered electron (BSE) imaging at <1 μm per pixel was derived for the studied inclusions. The homogeneity of inclusions after the experiment was confirmed by the analysis of glasses at 3 points. Thus, Tables S1, S5 contain the average compositions from three analyses carried out for each inclusion. The representative compositions of constituent phases are given in Table S2 and S3. Trace elements and volatile components were measured using an ion microprobe Cameca IMS-4F (SIMS) at the Valiev Institute of Physics and Technology of Russian Academy of Sciences, Yaroslavl Branch RAS (IMT YB, analysts S.G. Simakin, E.V. Potapov) according to the literature method (Nosova et al., 2002 and Supplementary Text S1).

The determination of the major and trace elements in rocks was carried out by X-ray fluorescence and inductively coupled plasma–mass spectrometry performed at the Institute of Geology of Ore Deposits, Petrography, Mineralogy, and Geochemistry (IGEM RAS, analyst A.I. Yakushev) and the Institute of Microelectronics Technology and High-Pure Materials RAS (IPTM RAS) in Chernogolovka, Russia (analyst V.K. Karandashev). The conditions for performing analytical work were described in previous work (Karandashev et al., 2017).

RESULTS

Geology of the Maslovsky Deposit

The PGE-Cu-Ni Maslovsky deposit is located in the central part of the Norilsk syncline (Figs. 2a, 2b) and consists of two intrusive bodies. Previously, Krivolutskaya et co-authors (2012a) have indicated forming the Northern and Southern Maslovsky intrusions by two discrete magmatic pulses. Such a conclusion has been based on the variations in the Nb/Ta ratio of the gabbro-dolerites and different compositions of their clinopyroxene and olivine phenocrysts (Supplementary Figs. S1, S2). Figure 3 shows major and trace element compositions of the Northern and Southern intrusions. In general, both intrusions with MgO > 5 wt % are identical in compositions for all major and trace elements, excluding Nb/Ta (Th/Ta) ratio, which is higher in the Northern intrusions. However, it is noteworthy that in the range of MgO < 5 wt %, the set of Southern intrusions compositionally differs from the rest of the Maslovsky intrusions by higher SiO_2, TiO_2, FeO*, Na_2O, K_2O, P_2O_5, REE, HFSE, Ba, Th, U, Y and low Al $_2O_3$, CaO. We believe that such differences cannot be explained by crystalline fractionation of main minerals presented in intrusions and can indicate the presence of parental magmas of various compositions. This suggestion is proved by different trace element contents in rock-forming minerals of the Southern and Northern Maslovsky intrusions (Krivolutskaya et al., 2012a).

The northern part of the Maslovsky deposit is a continuation of the Norilsk 1 intrusion (Fig. 2c, borehole OM-4), and the southern part is an independent body, the maximum thickness of which reaches 412 m in borehole OM-24 (Fig. 2d). The detailed structure and mineralogical and geochemical features of the Maslovsky deposit were described in a previous study (Krivolutskaya et al., 2012a).

The intrusions have a differentiated structure typical of the intrusions of the Norilsk complex, where high-magnesium rocks are localized in the lower part, and more acidic ones occur in the upper part. Gabbro-dolerites dominate in the intrusion; they have varying olivine contents and are subdivided into the following horizons (from top to bottom, Ol vol %): olivine-free, olivine-bearing (3–5%), olivine (5–20%), picritic (40–60%), and taxitic (3–15%). The upper parts of the intrusions are composed of gabbro-diorites, ferrogabbro, and leucogabbro (sections OM-24 and OM-4, Figs. 2c, 2d). Plagioclase, olivine, and clinopyroxene are the main rock-forming minerals, with different compositions along the section, reflecting the variations of the rock compositions (Krivolutskaya et al., 2012a).

The Southern Maslovsky massif breaks through the tuff-lava rocks, namely, the Ivakinsky–Nadezhdinsky Formations, occupying the highest position in the stratigraphic section compared with the other ore-bearing intrusions. It differs from the Northern Maslovsky intrusion (Figs. 2c, 2d) by the occurrence of the thick horizon of taxitic gabbro-dolerites (35 m) in its lower part, which is practically absent in the latter massif. Furthermore, it comprises a thin horizon (25 m) of high-magnesium rocks (picritic gabbro-dolerites), which takes only 10% of gabbro-dolerite section, while in the Northern Maslovsky intrusion, high-Mg varieties compose up to 50% of the section. A characteristic feature of the Southern Maslovsky intrusion is an occurrence of unusually thick horizon (180 m) "prismatic-granular" gabbro-dolerites (corresponding to olivine-bearing gabbro-dolerites), where clinopyroxene forms idiomorphic crystals and, together with plagioclase, is located in the fine-grained bulk groundmass (altered glass).

Morphology and size of olivine crystals in the rocks (Fig. 4) vary from large idiomorphic grains 0.5–1 mm (Figs. 4a, 4b, 4g, 4h) to small round grains 0.2–0.3 mm (Figs. 4c–4f) included in clinopyroxene. Olivine and clinopyroxene phenocrysts in the Maslovsky intrusions display notable compositional diversity between the Northern and Southern intrusions, even at similar forsterite or Cpx Mg# range (Supplementary Figs. S1, S2). Olivines from the Southern intrusion are characterized by higher CaO (Fig. S1A), Cr_2O_3 (Fig. S1C), Al_2O_3 (Fig. S1D), and lower NiO (Fig. S1B), contents in comparison with the Northern intrusion olivines within the range of $Fo_{81\text{-}76}$.

Clinopyroxene from the Southern intrusion is enriched in TiO_2 (Fig. S2B), Al_2O_3 (Fig. S2C), CaO (Fig. S2D), Na_2O (Fig. S2E), Cr_2O_3 (Fig. S2F), and depleted in SiO_2 (Fig. S2A) with respect to the Northern intrusion clinopyroxenes (Cpx) within the range of Mg# 85–80. The high rate of magma cooling in the Southern intrusion also affects the structure of minerals: numerous melt inclusions can be observed. In this work, we selected (1) a picritic gabbro-dolerite (sample OM-24/814), where olivine is an early phase and contains information on the most primitive melt which formed this massif, and (2) a prismatic-granular gabbro-dolerite, where the largest inclusions in Cpx were found (sample OM-24/666) (Fig. 2d).

Magmatic Inclusions in Rock-forming Minerals from the PGE–Cu–Ni Maslovsky Deposit

Magmatic inclusions in olivine. As mentioned above, olivine crystals are the earliest liquidus phases in high-Mg rocks of the Norilsk intrusions, i.e., in picritic gabbro-dolerite. This rock (sample OM-24/814) is dark-gray and medium-grained with a massive structure and panidiomorphic or poikilitic texture (Fig. 4). It consists of the following (vol %): olivine $Fo_{77.8–80.2}$ (60–70) clinopyroxene Mg# 70.1–84.3 (15–18) (Supplementary Table S1), plagioclase $An_{66.1–80.3}$ (20–30), Cr-magnetite-spinel (6.1–33.4 wt % Cr_2O_3) (up to 5), and orthopyroxene (1–2), ilmenite (<1), sulfides

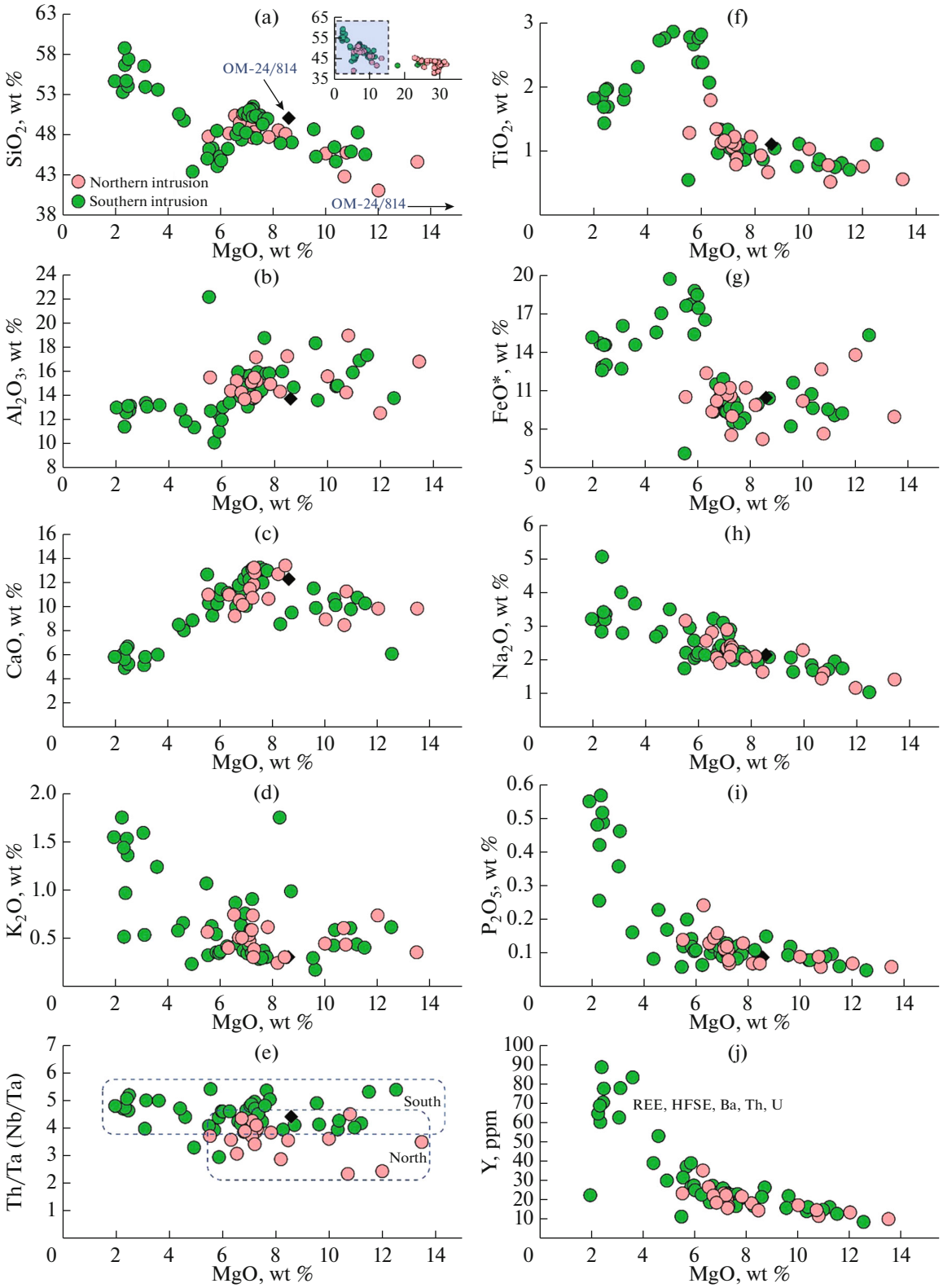

Fig. 3. Diagrams MgO–SiO_2 (a), Al_2O_3 (b), CaO (c), K_2O (d), Th/Ta (e), TiO_2 (f), FeO (g), Na_2O (h), P_2O_5 (i), Y (j) for rocks of the Southern and Northern intrusions of the Maslovsky deposit.

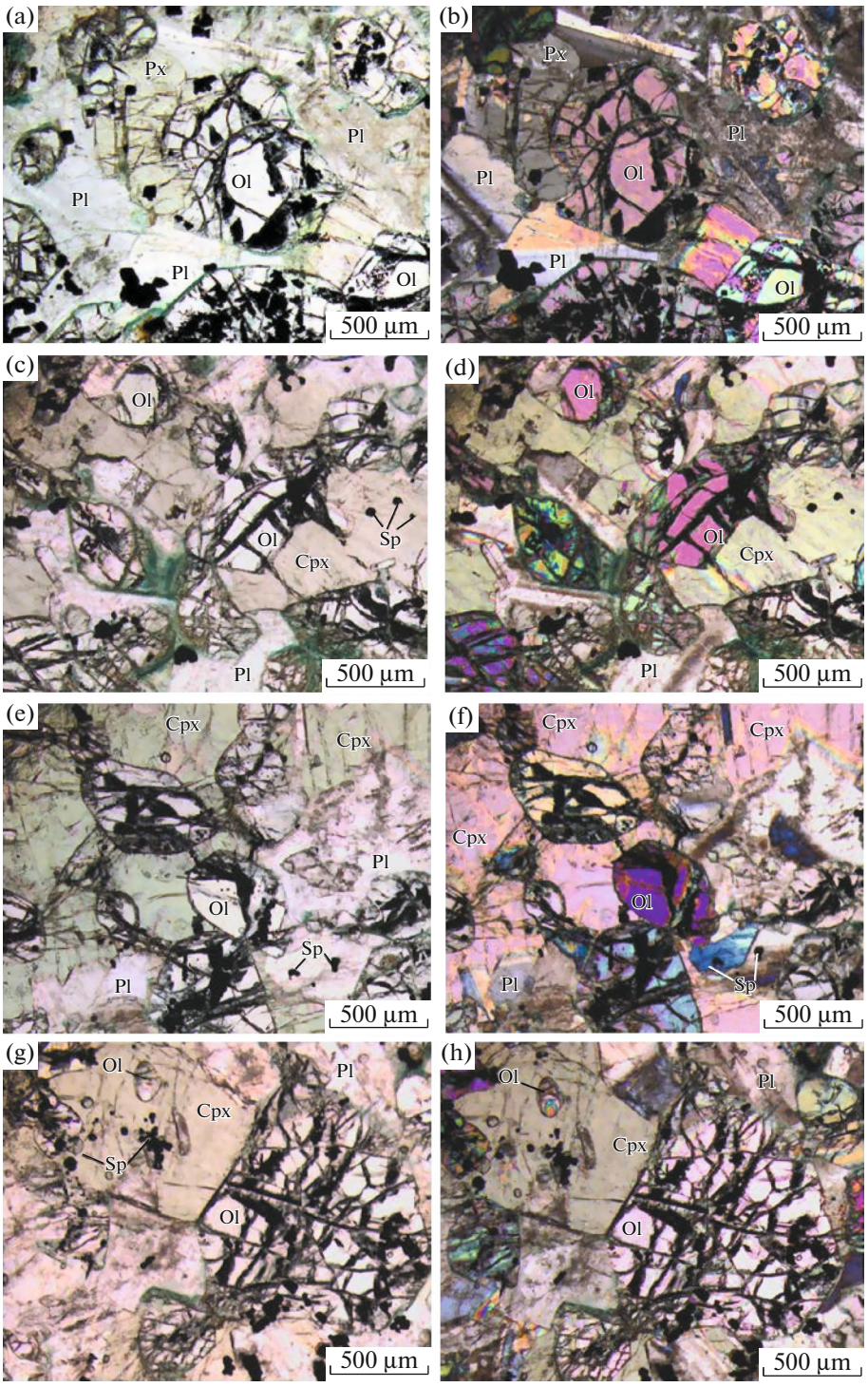

Fig. 4. Microphotographs of picritic gabbro-dolerite from the Maslovsky deposit (sample OM-24/814). Olivine grains in clinopyroxene and plagioclase: (a) one nickole; (b) crossed nickoles. (c–f) Poikilitic texture forming small, rounded olivine grains in large clinopyroxene and plagioclase grains (e) one nickol, (f) crossed nickols). Intergrowth of large olivine and clinopyroxene crystals: (g) one nickole; (h) crossed nickols.

Here and in Fig. 5: Ol—olivine, Cpx—clinopyroxene, Sp—spinel, Pl—plagioclase.

(0.1–0.2). Its chemical composition is as follows (wt %): 41.65 SiO_2, 0.64 TiO_2, 8.14 Al_2O_3, 15.32 Fe_3O_3, 0.22 MnO, 23.74 MgO, 6.01 CaO, 0.81 Na_2O, 0.23 K_2O, 0.06 P_2O_5, 0.59 Cr_2O_3, and 2.00 LOI.

Magmatic inclusions in olivine (Figs. 5a–5l) are represented by glassy melt inclusions (Fig. 5b), partially crystallized (Figs. 5b, 5h, 5i) or completely crystallized inclusions (Figs. 4c, 4g), fluid (Figs. 5f, 5l),

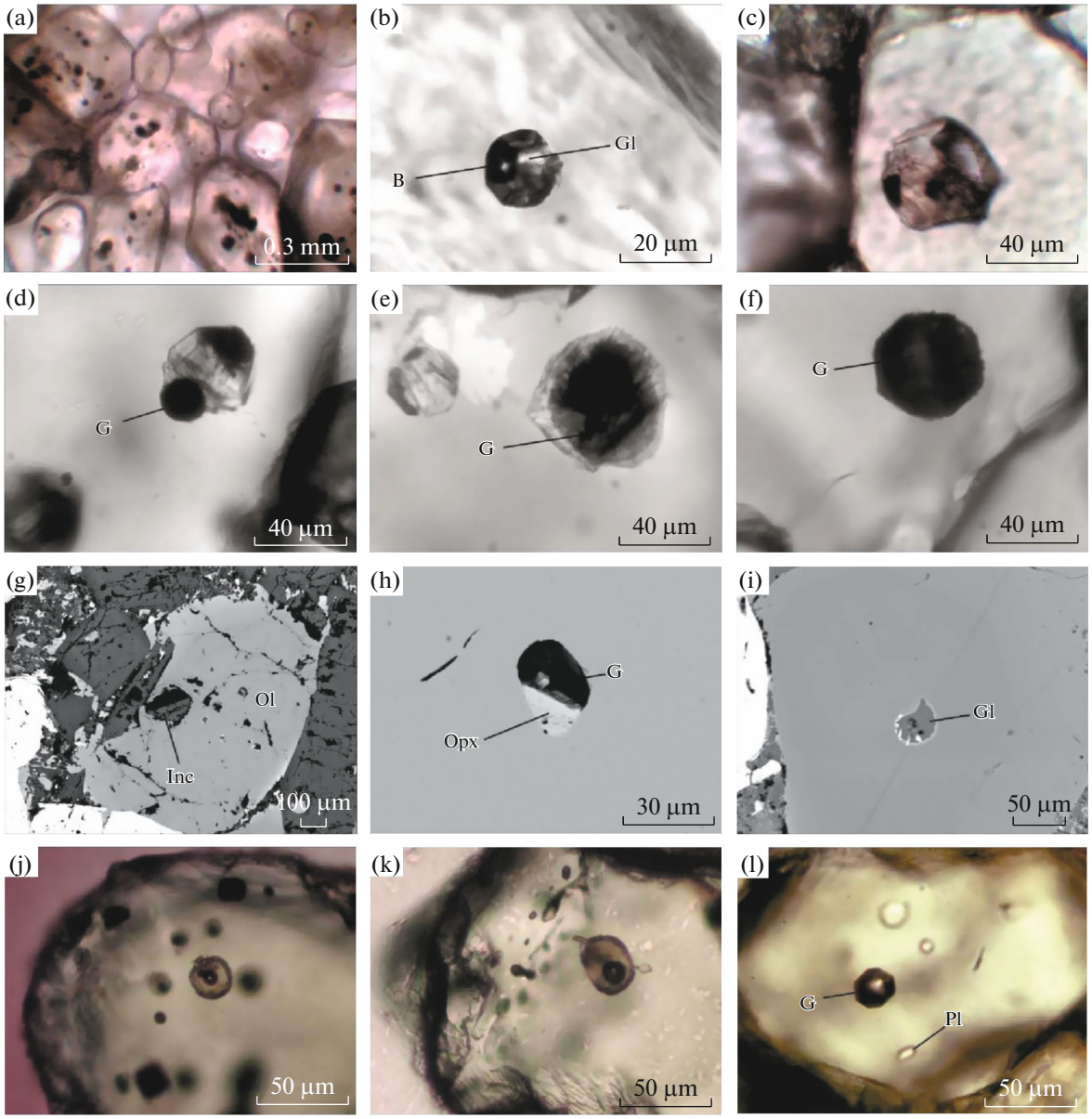

Fig. 5. Microphotographs of the inclusions in olivines from picritic gabbro-dolerites. (a) Granular olivine with numerous melt inclusions (black spots), (b) partially crystallized melt inclusion, (c) completely crystallized melt inclusion, (d) combined inclusion (fluid + melt), (e) fluid inclusion with crystalline border, (f) gas inclusion, (g) melt inclusion in olivine, backscattered electron (BSE) image; (h) inclusion on the surface of polished olivine, (i) melt inclusion in olivine, BSE image, and (j–l) quenched melt inclusions in olivine after the experiment Opx—orthopyroxene, Inc—inclusion, Gl—glass.

crystalline (mostly plagioclase, Fig. 4l), or combinations of all these phases (Krivolutskaya, 2016). Melt inclusions account for 80% of the volume of all inclusions. Small melt inclusions (10–12 μm) are glassy (Figs. 5b, 5i) as usual, while large inclusions (40–85 μm) are recrystallized (Fig. 5c). Orthopyroxene, ilmenite, and pyrrhotite are observed as daughter minerals. The simultaneous presence of primary fluid and melt inclusions in the mineral (Figs. 5e, 5l) indicates the saturation of magma with volatile components.

The problem with the homogenization of melt inclusions in olivines was caused by the growth of magnesium olivine (Table S2) during the experiment (Krivolutskaya et al., 2012a) (eight inclusions, Table S1). To get rid of the new phases, inclusions were exposed for a longer time at high temperatures (1100–1200°C) as usual. Nevertheless, this problem could not be completely overcome (the newly formed small olivine crystals are visible, as shown in Figs. 5j, 5k); the composition of experimentally quenched glasses corresponds to a bit more evolved olivine-fractionated melt.

The variations of experimentally obtained glasses in olivines (Table S1) show a simultaneous decrease in MgO content from 9.34 to 6.31 wt % and an increase

in almost all components in the melt, including Al_2O_3, TiO_2, SiO_2, Na_2O, K_2O, P_2O_5, FeO, and Cl (Figs. S3A, C–I), except CaO and S (Figs. S3B, J). In addition, the inclusions in olivines from these samples contain <0.1 wt % chlorine concentrations, except for one analysis (0.25 wt %).

Magmatic inclusions in clinopyroxene. Clinopyroxene in the rocks of the Norilsk intrusions crystallizes mostly as the late liquidus phase. As a rule, it contains small inclusions (5–10 μm) confined to cleavage planes, which do not allow termination of melt compositions. Hence, rocks in the upper part of the Southern Maslovsky intrusion, where clinopyroxene is an early phase and contains numerous large melt inclusions, are rare and very suitable for experimental work.

We studied a sample taken at a depth of 666 m (sample OM-24/666). The rock has a massive, sometimes planar parallel structure and porphyric, ophitic texture. It contains largely elongated (up to 5–6 mm) plagioclase and clinopyroxene crystals and rare isometric olivine grains (0.2–0.3 mm) (Figs. 6a, 6b). Fined-grained interstitial mass (up to 10% of the rock volume, Figs. 6a–6d) contains dendritic titanomagnetite crystals (Fig. 6), fine grains of quartz, potassium feldspar, sometimes with an increased Ba content (Table S3), fluorapatite, Sr-apatite, and phlogopite. There are pyrrhotite, chalcopyrite, and pyrite (up to 1% in total). The composition of clinopyroxene varies from Mg# 76–77 in the central zones of grains to Mg# 72–73 in the peripheral ones. A similar zonation is also typical of plagioclase (Table S3).

Results of this rock's major and trace element analysis showed agreement with typical traps excepting MgO, especially the Morongovsky basalts. It has the following composition (wt %): 50.15 SiO_2, 1.09 TiO_2, 13.74 Al_2O_3, 11.62 Fe_2O_3, 0.21 MnO, 8.59 MgO, 12.30 CaO, 2.15 Na_2O, 0.31 K_2O, and 0.09 P_2O_5 (Table S5).

All rock-forming minerals (olivine, clinopyroxene, and plagioclase) are characterized by the presence of melt inclusions (Figs. 6a, 6b), the best of which occurs in clinopyroxenes. Clinopyroxene crystals contain large partially crystallized inclusions, the content reaching 5 vol % of the mineral. The central parts of the crystals are most saturated with them. The size of inclusions ranges 20–80 μm, and they have a prismatic shape or rhombic in thin sections (Figs. 6c, 6e), sometimes they are elongated (Figs. 6f, 6h) and irregular form (Fig. 6g). The clinopyroxene crystals with large inclusions (Figs. 7a, 7b) are enclosed by glass with skeletal titanomagnetite crystals (Fig. 7c) and associated with zoned plagioclase (Figs. 7b, 7d). Inclusions consist of glass (80–90 vol %), titanomagnetite (5–10%), and spinel (hercynite) (5–10%) (Figs. 7, 8). Crystallization of Fe-rich clinopyroxene (Mg# 48.0) on the walls of the inclusions is visible in back-scattered electrons images, while the host pyroxene has Mg# 74.5 (Figs. 7e, 7f). Titanomagnetite forms crystals with six or four edges in a section, it is overgrown with hercynite. They are located along the inclusion boundary with the host mineral (Figs. 7e, 7f). The composition of melt inclusions in detail is shown in Figs. 8a–8o, where the maps of element distributions in characteristic X-rays for two melt inclusions are given. The first inclusion consists (Fig. 8a, backscattered electron image) of 70% glass (Gl), titanomagnetite crystal (Ti-Mag) in its center part, and two small (2 and 5 μm) rhombic hercynite crystals (Hc). The light border around the inclusion shows more Fe-rich clinopyroxene than host-clinopyroxene. Al and Na distributions fix the glass in host-clinopyroxene (Figs. 8b, 8c), while Mg and Ca contents (Figs. 8d, 8e) show inclusion depletion in these elements. Elevated Fe, V, Ti concentrations (Figs. 8f, 8g, 8h) demonstrate titanomagnetite occurrence and, partially, hercynite (Fig. 8f). It seems there are two tiny sulfides in the inclusion (Fig. 8i). The second inclusion (Figs. 8j–8o) has a more complicated structure than the first inclusion, although it consists of the same minerals. The glass of this inclusion (70 vol %) comprises 5 titanomagnetite crystals and one large lamellar crystal (50 μm). Figs. 8k, 8l reflect high Al and Si concentrations in the glass of melt inclusion, respectively, and Fig. 8m shows Fe-rich phases (titanomagnetite and hercynite). The melt inclusion depletions in Mg and Ca are shown in Figs. 8n, 8o. The compositions of the phases are shown in Table S4.

The homogenization temperatures (T_{hom}) of individual inclusions in clinopyroxenes vary from 1170 to 1190°C, determined during the heating of inclusions at the Sobolev–Slutsky stage. It depends on the Mg# number of pyroxene. After T_{hom} determination, many pyroxene grains were simultaneously heated in a high-temperature vertical furnace at T = 1190°C with QFM. Most inclusions exhibited complete homogenization, i.e., represented only by glass. Some inclusions were partially homogenized because small bubbles were observed in the glass. They are marked as "b" in Supplementary Table S5. Two inclusions in olivine from this sample were studied as well.

Analysis of experimental quenched glasses (Table 1, Table S5) demonstrates variations in major oxides that reflect the fractionation crystallization of the primary melt (Figs. 9a–9j). The reduction in CaO content from 12.48 to 9.90 wt % (Fig. 9c) together with decreasing MgO content from 7.18 to 5.23 wt % showed clinopyroxene crystallization (Ol-Cpx cotectic) during a temperature decrease. Simultaneously, the melt was enriched in (wt %): Al_2O_3 (10.61–12.96 or 10.61–12.96; Fig. 9b), Na_2O (1.43–3.22; Fig. 9f), K_2O (0.44–0.75; Fig. 9i), and P_2O_5 (0.13–0.23; Fig. 9g). TiO_2, Cl (Figs. 9d, 9j), and H_2O behaviour weakly depends on MgO. The Cl content increases with K_2O content.

However, some differences were observed in the composition of rocks and inclusions when analyzing the ratios of a number of elements characterizing the

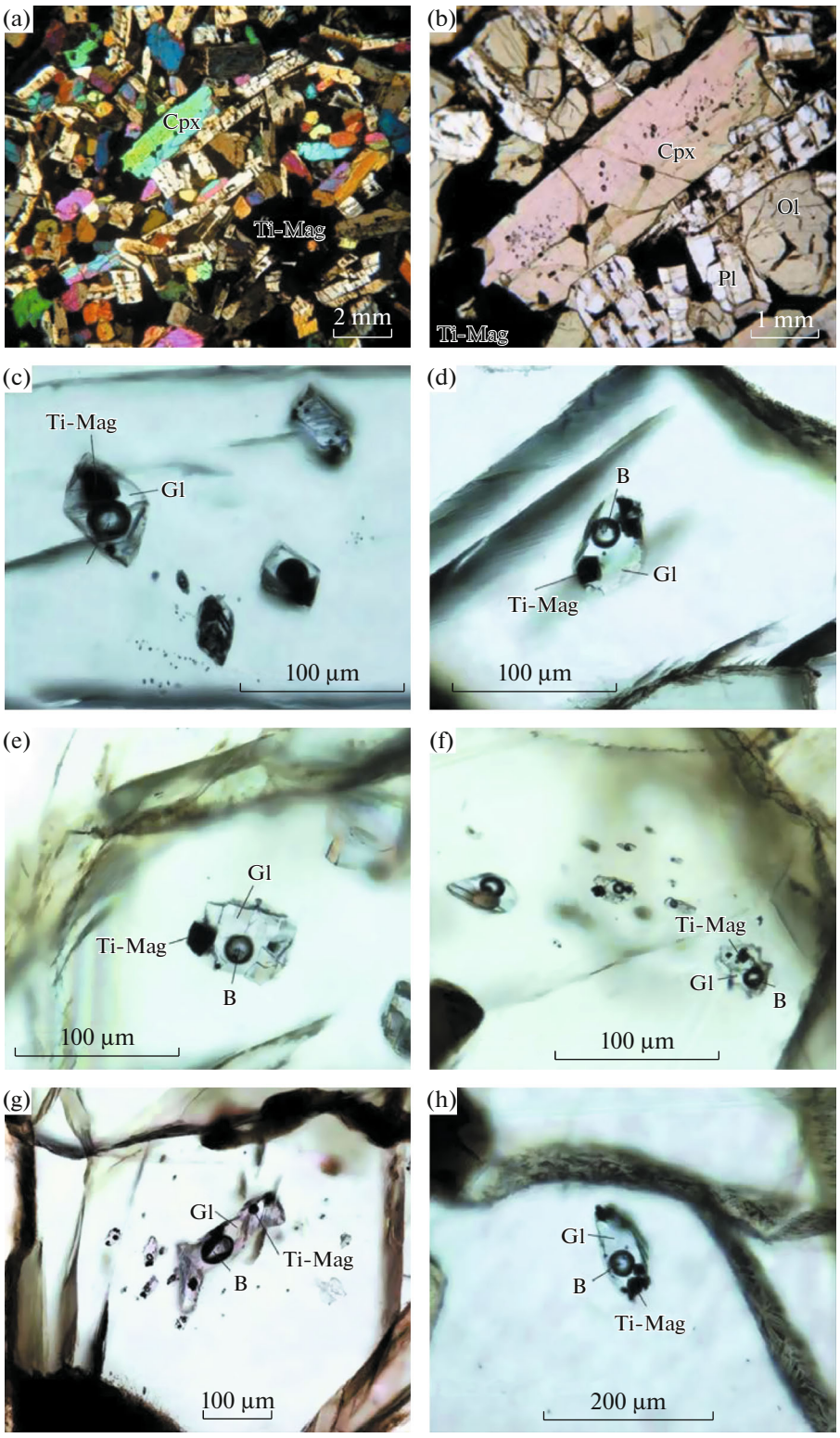

Fig. 6. Microphotographs of the inclusions in clinopyroxenes (sample OM-24/666). (a) Texture of rocks, (b) a large grain of pyroxene with many melt inclusions (black), (c) five melt inclusions of prismatic shape, (d) inclusion with some crystals of titanomagnetite (or/and hercynite) and bubble, (e) inclusion with one crystal of titanomagnetite and bubble, (f) some melt inclusions in one plane, (g) one large inclusion of irregular shape and some small melt inclusions, and (e) elongated melt inclusion with some crystals of titanomagnetite (or/and hercynite) and bubble. Cpx—clinopyroxene, Pl—plagioclase, Ol—olivine, Ti-Mag—titanomagnetite, B—bubble, Gl—glass.

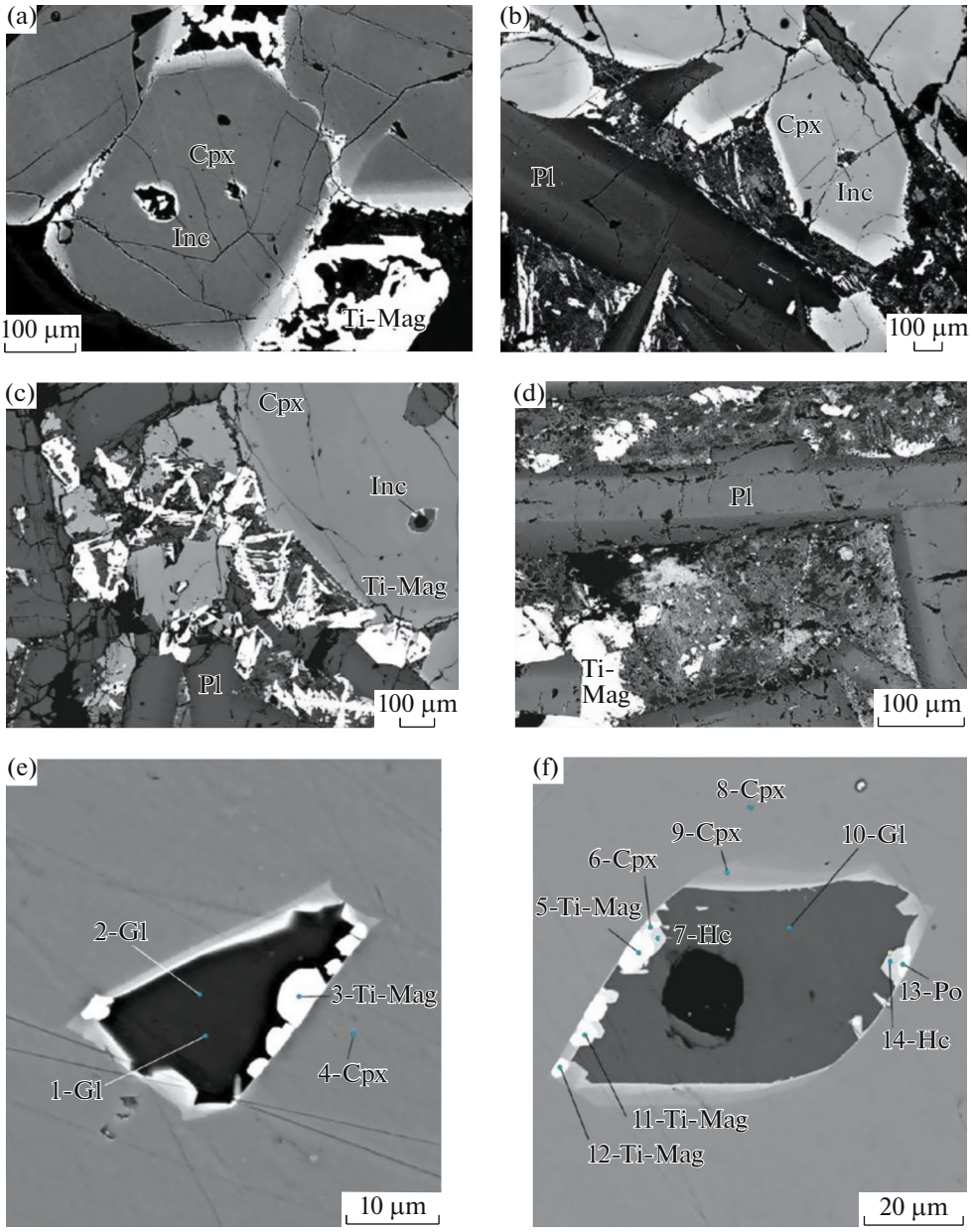

Fig. 7. Backscattered electron images of rocks and clinopyroxenes with melt inclusions. (a) Idiomorphic crystal of pyroxene with two melt inclusions, (b) plagioclase and pyroxene (with melt inclusions) with fine-grained basis, (c) pyroxene crustal with melt inclusion and titanomagnetite dendritic crystals in the groundmass, (D) plagioclase crystals and fine-grained groundmass, and (e, f) melt inclusions with mineral phases near their surface. Cpx—clinopyroxene, Pl—plagioclase, Ti-Mag—titanomagnetite, Gl—glass, Hc—hercynite. The point number corresponds to the analysis number in Table S4.

slope of the spectrum and the magnitude of the Ta–Nb anomaly (Figs. 10a–10f). In general, the spectra of the inclusions in clinopyroxenes differ by a smaller angle of inclination relative to the X-axis compared to rocks and basalts, which follows from Figs. 10e, 10f and Fig. S4 for olivines. By the magnitude of the Ta–Nb anomaly, the compositions of melts in inclusions are very close to both gabbro-dolerites and basalts. The rocks are also typically more enriched in uranium than melts.

The Parental Melt Compositions of the Southern Maslovsky Intrusion

We used the data on inclusions in both clinopyroxenes and olivines to estimate the composition of the parental magma of the Maslovsky intrusion.

First, we have checked the equilibrium of melt inclusions in clinopyroxenes with their host minerals. Temperature (T) and pressure (P) crystallization were

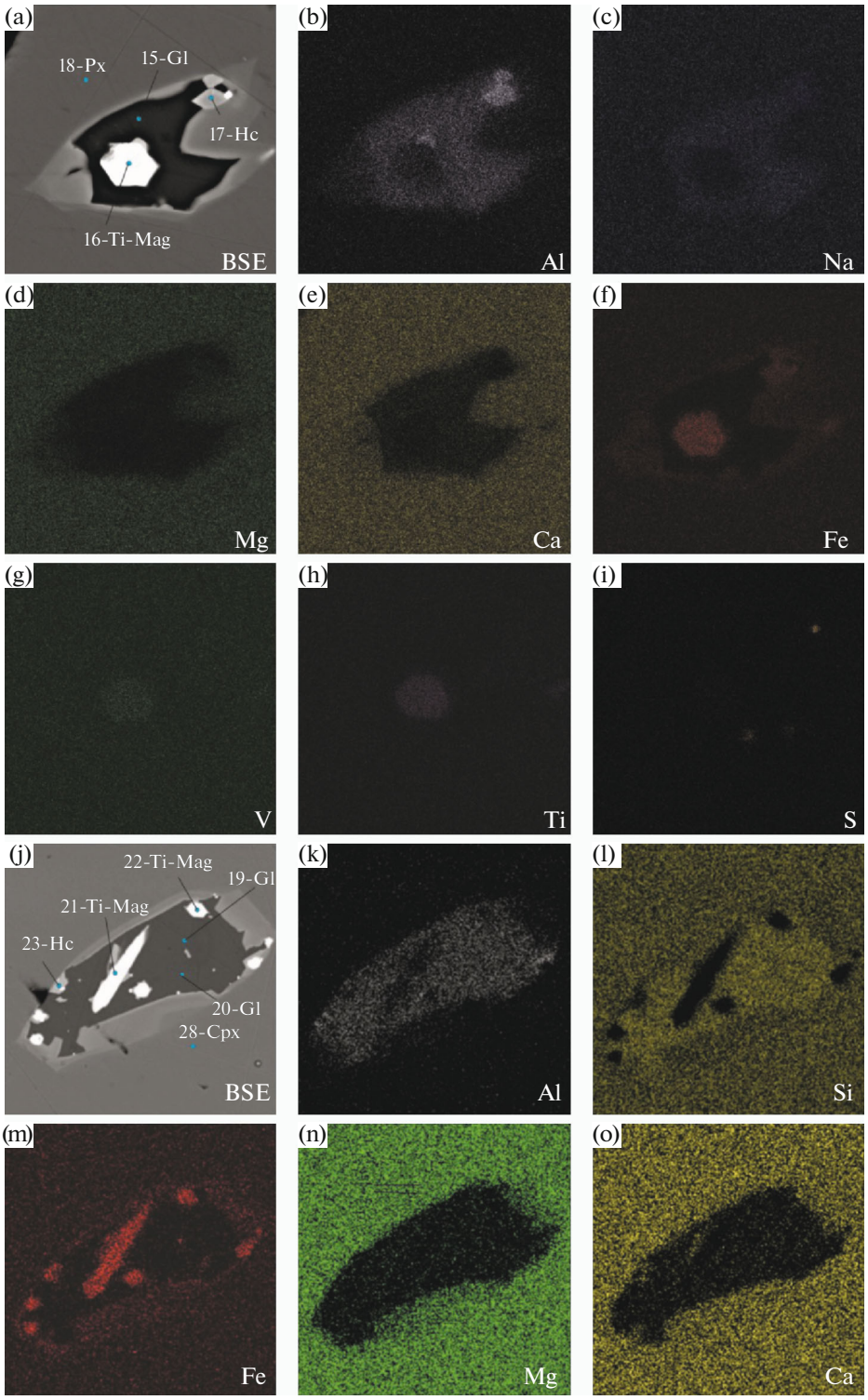

Fig. 8. Backscattered electron images of melt inclusions in clinopyroxenes (a, j) and their maps in characteristic X-ray. b, k: Al K_α; c: Na K_α; d, n: Mg K_α; e, o: Ca K_α; f, m: Fe K_α; g: V K_α; h: Ti K_α; i: S K_α; l: Si K_α.

calculated after (Putirka, 2008). The T average is 1205°C, and P is 2.9 kbar. Tests for an equilibrium between clinopyroxene and a nominal coexisting liquid can be made by comparing observed and predicted values for Fe–Mg exchange, or K_D(Fe–Mg) Cpx-liq, which should be 0.27 ± 0.03 (Ford et al., 1983). For this test, compare the values in column Z (Supplementary Table S6, sheet 2) to 0.27. In Column Z, a coefficient is used so that the amount of Fe in the liquid is only Fe^{2+}, not Fe^{3+}.

Table 1. Representative compositions of melt inclusions in pyroxene

No. mi	1a	6a	26a	34a	35a	46a	59a	78a
Size, μm	40	30	40	50	30	70	60	30
SiO_2	51.92	49.57	51.10	49.00	50.74	50.64	49.02	51.87
TiO_2	1.60	1.83	1.80	1.87	1.61	1.56	1.57	1.94
Al_2O_3	12.66	12.25	12.42	11.74	12.76	11.47	11.45	12.43
FeO	13.27	15.11	14.13	14.42	13.84	13.58	14.08	12.73
MnO	0.21	0.27	0.23	0.26	0.24	0.22	0.24	0.23
MgO	5.79	5.82	5.73	6.74	5.80	6.78	6.80	5.94
CaO	10.45	10.33	10.34	11.44	10.53	11.28	11.43	10.47
Na_2O	3.11	3.08	2.98	2.71	3.03	2.77	2.77	3.17
K_2O	0.70	0.67	0.61	0.55	0.63	0.61	0.62	0.61
P_2O_5	0.21	0.21	0.20	0.17	0.19	0.17	0.19	0.20
S	0.11	0.13	0.08	0.13	0.10	0.10	0.09	0.10
Cl	0.14	0.22	0.13	0.12	0.13	0.13	0.16	0.19
Total	100.18	99.48	99.73	99.14	99.61	99.31	98.41	99.87
Rb	34.0	34.9	31.8	28.4	32.0	30.2	31.4	33.3
Sr	243	213	222	220	215	202	203	186
Zr	126	142	124	122	115	119	121	134
Ba	238	217	210	196	203	194	202	192
Ce	28.0	29.1	26.6	27.7	24.8	24.5	24.6	25.4
Sm	5.04	5.49	4.56	4.99	4.44	4.40	4.59	5.44
Er	4.29	5.56	4.42	4.67	4.01	4.12	4.33	5.05
Ta	0.43	0.38	0.38	0.42	0.37	0.38	0.40	1.11
Th	1.34	1.43	1.27	1.24	1.22	1.19	1.18	1.15
U	0.53	0.52	0.51	0.45	0.49	0.44	0.44	0.47
Pb	4.14	4.70	3.80	4.12	4.04	3.21	4.76	3.92
Hf	3.57	3.82	3.69	3.63	3.19	3.04	3.43	4.18
Lu	0.58	0.67	0.62	0.66	0.53	0.58	0.66	0.71
Dy	5.91	7.02	6.02	6.51	5.51	6.01	5.97	6.66
Gd	5.68	7.42	5.89	5.42	5.85	5.06	5.18	5.31
Nd	17.0	19.2	15.9	17.2	15.5	15.1	16.5	17.7
Pr	3.49	3.80	3.19	3.51	3.06	3.02	3.16	3.38
La	12.1	12.1	10.9	11.7	10.1	9.90	10.9	10.7
Cs	0.68	0.57	0.57	0.39	0.52	0.53	0.55	0.62
Nb	7.24	7.43	6.72	7.26	6.06	5.79	6.13	6.03
Y	34.2	41.2	35.3	39.8	34.0	37.3	35.4	39.7
Yb	3.72	4.53	3.98	4.28	3.70	3.87	4.09	4.63
Eu	1.77	1.83	1.62	1.66	1.42	1.42	1.52	1.57
B	4.44	5.47	4.77	4.52	4.48	4.83	4.92	5.46
Li	0.58	0.66	5.91	6.74	5.16	6.75	10.07	5.16
Be	5.12	4.76	0.67	0.68	0.63	0.61	0.61	0.63
H_2O	0.19	0.33	0.27	0.31	0.33	0.28	0.21	0.21
F	0.054	0.045	0.048	0.05	0.05	0.049	0.045	0.046
Cpx Mg#, Fo, mol %	73.8	74.0	76.0	76.8	76.4	76.3	75.0	66.6

Oxides, H_2O, and F, are given in wt %, elements—in ppm. No. 78a—inclusion in olivine.

Fig. 9. Harker diagrams for melt inclusions in olivine and clinopyroxene MgO–SiO_2 (a), Al_2O_3 (b), CaO (c), TiO_2 (d), FeO (e), Na_2O (f), P_2O_5 (g), K_2O (h), S (i), Cl (j). Data in Tables S1, S5. Green field shows the rock compositions of the Southern Maslovsky intrusion (data after Krivolutskaya et al., 2012). Circles: yellow—inclusions in clinopyroxene, sample OM-24/666; blue—inclusions in olivine, sample OM-24/814; red—inclusions in olivine, sample OM-24/666. Black rhomb—composition of sample OM-24/666. Stars—parental melt compositions calculated based on the inclusions in Cpx (OM-24/666, yellow) and in olivines (OM-24/666, red; OM-24/814, black).

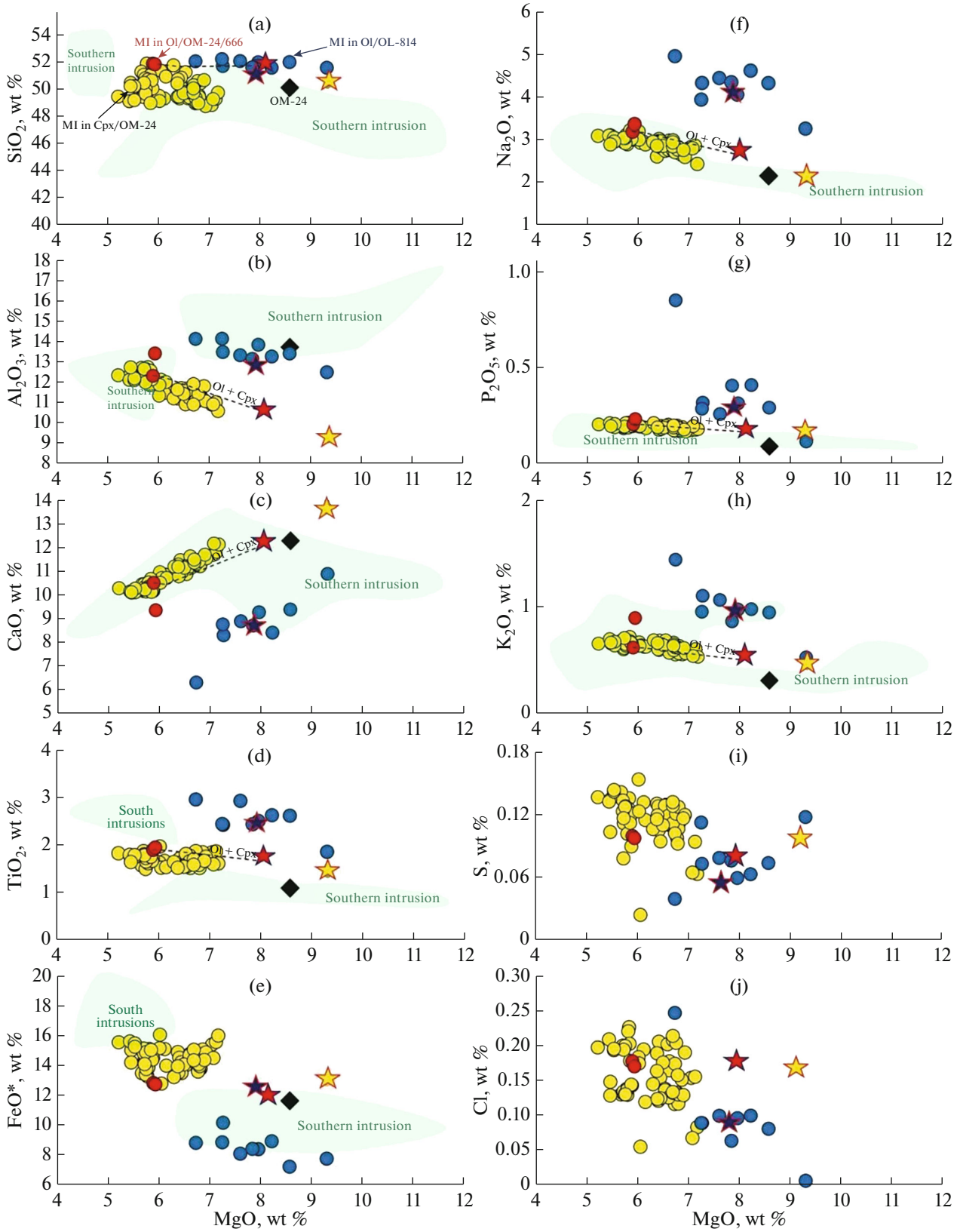
(a)
SiO2, wt %
MI in Ol/OM-24/666
MI in Ol/OL-814
Southern intrusion
OM-24
MI in Cpx/OM-24
Southern intrusion
(b)
Al2O3, wt %
Southern intrusion
Southern intrusion
Ol + Cpx
(c)
CaO, wt %
Ol + Cpx
Southern intrusion
(d)
TiO2, wt %
South intrusions
Ol + Cpx
Southern intrusion
(e)
FeO*, wt %
South intrusions
Southern intrusion
MgO, wt %
(f)
Na2O, wt %
Ol + Cpx
Southern intrusion
(g)
P2O5, wt %
Ol + Cpx
Southern intrusion
(h)
K2O, wt %
Ol + Cpx
Southern intrusion
(i)
S, wt %
(j)
Cl, wt %
MgO, wt %

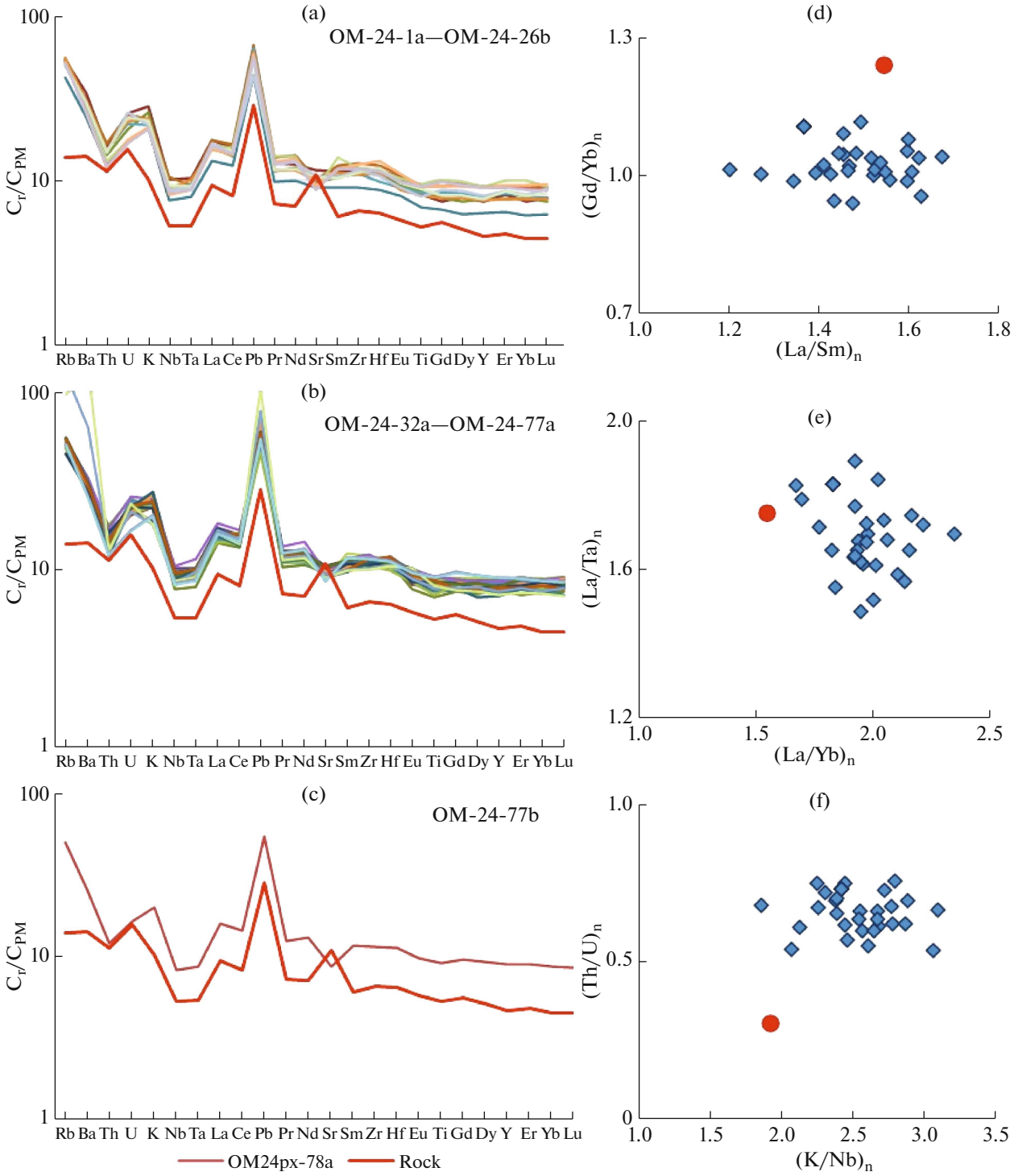

Fig. 10. Spider diagrams for melt inclusions in clinopyrones, host rock (red line). Diagrams $(La/Sm)_n$ vs $(Gd/Yb)_n$ (d), $(La/Yb)_n$ vs $(La/Ta)_n$ (e), and $(K/Nb)_n$ vs $(Th/U)_n$ (f) for melt inclusions in clinopyroxenes (blue rhombs) and host-rock (OM-24/666) (red circle).

Another test was used to compare predicated and observed values for the clinopyroxene components. For experimental data, various quantities that can be used as tests for equilibrium appear to be correlated; thus, if equilibrium or disequilibrium is indicated by one parameter, other parameters often (though no always) follow. However, in the RiMG volume (Putirka, 2008), we show some instances for experimental data where the comparison of clinopyroxene components provides a more certain test than for

K_D(Fe–Mg)cpx-liq (Supplementary Table S6). Most of the inclusions are in equilibrium with host clinopyroxenes. Their compositions were calculated to be in equilibrium with the most magnesium clinopyroxene Mg# 85 in the Southern intrusion (Table S7).

The composition of the melt inclusions in olivines from both samples OM-24/666 and OM-24/814 were recalculated to equilibrium with their host olivines. To get the primary melt composition for the Southern Maslovsky intrusion, we calculated it to equilibrium with the most magnesium olivine found in this intrusion (Fo = 80.9) using the PETROLOG-3 computer program (Danyushevsky and Plechov, 2011). Also, the inclusion of olivine in sample OM-24/666 No 78a was calculated to the host olivine and subsequent reverse crystallization of the cotectic to $Fo_{80.9}$ at 3 kbar. These data are given in Table S6.

The difference in primary melts (1 and 2 for OM-24/666 and OM-24/814) (Fig. 10, Fig. S4) i. e. enrichment in many components of the second one, for picritic gabbro-dolerites,—TiO_2, Al_2O_3, Na_2O, K_2O, P_2O_5, may be partially due to the occurrence of olivine crystals in inclusions. However, this melt contains low CaO, FeO, S, and Cl contents; thus, it differs from the primary melt-1 of the upper part of the intrusion. The structure of the Norilsk intrusions reflects their complex formation. Likhachev demonstrates (Likhachev, 1965, 2006, 2019) that inhomogeneous magma intruded in the modern chamber: two magma portions were represented by enriched in olivine and plagioclase melts (that formed picritic and taxitic gabbro-dolerites, consequently), and one consisted of pure melt (which produced olivine-bearing gabbro-dolerites – gabbro-diorites). Thus, two primary melts correspond to different magma portions. The primary melt-2 for picritic gabbro-dolerite of the Maslovsky deposit is close to obtained primary melt for the picritic gabbro-dolerite of the Talnakh intrusion (Krivolutskaya and Sobolev, 2001).

The volatile contents (water, chlorine, sulfur, and fluorine) in magmas before their eruption to the surface are of the greatest interest to us. The chlorine content is quite high in inclusions in pyroxenes, varying from 540 to 2260 ppm, averaging at 1550 ppm. However, the clinopyroxene-hosted melt inclusions may not belong to primary melts, they characterize evolved melt. The primary contents calculated in the olivine-hosted melt inclusions differ in two samples OM-24/666 and OM-24/814—1319 ppm and 940 ppm (Table 2). The latter content is close to the Cl contents for picritic gabbro-dolerites from the Talnakh and Zeleneya Griva intrusions (800–900 ppm Cl) (Krivolutskaya and Sobolev, 2001).

Sulfur concentrations vary in inclusions in clinopyroxenes, from 240 to 1540 ppm, and olivines, from 600 to 1110 ppm, on average 740 ppm in primary melt-1. According to data of (Haughton et al., 1974) melt-1 was not saturated with sulfur (Fig. S5). The primary melt-2 containing 1200 ppm S was saturated in sulfur, supported by mineralogical data because abounded sulfide globules occur in the rock.

The maximum measured water content in melt inclusion in clinopyroxenes is 4500 ppm; ordinarily, it ranges from 1100 to 3000 ppm. Therefore, it seems that water was partially lost. It can be estimated in this melt by an element of close incompatibility, namely, cerium ($H_2O/Ce = 168$ (Koleszar et al., 2009). The calculated values (Table 2) range from 3706 to 4979 ppm, averaging 4355. Thus, the maximum water content measured in clinopyroxene-hosted inclusion is close to its initial amount in the magma. Olivine-hosted melt inclusions contain 1370–2130 ppm H_2O.

Fluorine concentrations in inclusions in pyroxenes vary from 208 to 611 ppm, averaging 450 ppm. CO_2 content was also indirectly estimated by the element of close incompatibility, i.e., niobium. Taking the ratio $CO_2/Nb = 240$ in MORB (Saal et al., 2002), we obtain from 1305 to 1797 ppm (average 1487 ppm). It could be lost during magma ascent, and its content was lower during magma crystallization. B concentrations range from 3.30 to 8.24 ppm (average 4.86 ppm).

Thus, the volatile contents for the parental melt-1 (OM-24-666), are as follows (wt %): H_2O: 0.45; CO_2: 0.15%; Cl: 0.132; S: 0.0743; F: 0.045; B: 0.0005 (from 8.24 ppm to 3.30, av 4.86).

Estimation of Gases' Fluxes Released during the Traps Eruption

Estimating of the volume of traps is difficult because they are significantly eroded, especially in Taimyr and the south of the Tunguska syneclise. An ellipse can roughly outline their area of distribution with radii of 500 and 1100 km (including the dolerites' outcrops where lava flows are not supposedly preserved, Fig. 11a). The maximum thickness of the tuff-lava sequence can be estimated based on the preserved sections in synclinal structures (Fig. 11b), especially in the Kharaelakh syncline where 11 formations have been preserved. The lower formations are rift ones located only in the Yenisei-Khatanga trough or on its shoulders.

The Ivakinsky Formation (i.e., Syradasaysky in Taimyr) is widespread, with a volume of 39250 km^3 (if it occurs within the trough, there are no data). The three overlapping formations are distributed only in the Norilsk region and gradually pinch out to the Tunguska syneclise. The Syverminsky and especially the Gudchikhinsky Formations pinch sharply out to the Yenisei-Khatangsky fault. Their klin volume is 34500 km^3 ($a = c = 300$ km, $b = 230$ km, $h = 1$ km). Lower formations in the Norilsk form 73750 km^3 lavas (where the Nadezhdinsky tholeiitic basalts and tuffs take two-thirds of the volume). Although alkaline formations in the Maimecha-Kotuy area have a large thickness, they are restricted in spread (Vasil'ev et al.,

Table 2. Concentrations of volatiles in magmas and their masses

	1	2	3	4	5	6	7	8
Element	Maslovsky, incl. Cpx, ppm	Maslovsky average, ppm	Primary melt-1, ppm	Variations (Sibik et al., 2015)	Aver. (Sibik et al., 2015)	WPB (Naumov et al., 2017)	Mass of gases, Gt, Siberian Traps	Mass of gases, Gt/1 My, Arcs, (Fischer, 2008)
H_2O	1100–4297	2250	4500	–	–	1.18 wt %	53460	585000
Cl	537– 2263	1550	1319	3–511	98	1210	15670	5467
CO_2	1305–1797	1487	1279	1–891	181	950	15195	84920
F	208–607	450	387	1–848	157	1810	4598	228
B	3.30–8.24	4.86	4.18			10.4	49.7	–
S	245–1535	772	743	3–510	102	1030	9171	10080

1—measured volatile contents in inclusions in clinopyroxenes in the Southern Maslovsky intrusion, 2—average volatile contents in inclusions in clinopyroxenes in the Southern Maslovsky intrusion, 3—calculated volatiles contents in the primary melt-1 for the Southern Maslovsky intrusion, 4—variations volatile components in inclusions after (Sibik et al., 2015), 5—average volatile contents in inclusions after (Sibik et al., 2015), 6—volatile contents in within-plate magmas based on melt inclusions after (Naumov et al., 2017), 7—estimated masses of gases in the Siberian traps in gigatons, 8—data on volatile fluxes of modern arc volcanoes in gigatons calculated for 1 My (Fischer, 2008).

2017). Their volume is around 2000 km^3. The upper formations (from Morongovsky to Samoedsky, Tuklonsky is restricted in the area) have maximum 2200 m thickness (Lightfoot et al., 1993; Fedorenko et al., 1996). Their volume roughly equals rectangle square multiplied by thickness, i.e., 1000 km × 2200 km × 2 km = 4.4 million km^3. Taking 2.7 g/cm^3 density of basalt their weight is around 11.88 million Gt. Hence, the mass of the rift formations is around 0.45% of traps rocks in Eastern Siberia.

The masses of gases released during the traps eruption (Table 2) according to the data given above are roughly as follows (Tt): 53.5 H_2O, 15.2 CO_2, 15.7 Cl, 4.6 F, 9.2 S (18.34 SO_2), 0.05 B.

Basalt Magma Interaction with Sedimentary Rocks

Another possible source of gases during the Siberian traps formation is the underlying sedimentary rocks. Numerous gabbro-dolerite sills are located in the Cambrian-Permian carbonate-terrigenous rocks in the Siberian Platform and Taimyr. They are coeval with the formation of the Siberian flood basalts and belong to the same magmatic sources. Gases are released when hot magma intrudes sedimentary rocks, associated with the intrusions of the Katangsky complex that are widespread around the lava area, mostly bordering the Tunguska syneclise (Fig. 1a). Thick or thin (up to 450 m in the south of the syneclise or 2–20 m in its northwestern part, respectively) intrusive bodies of the Katangsky complex are located in the Cambrian-Devomian carbonate-terrigenous rocks (carbonate or evaporite) and coal-bearing terrigenous rocks of the Tunguska series (C_2–P_2). We studied these two relationships of intrusions with sedimentary rocks.

Basalt magma interaction with carbonate rocks. Contact of the gabbro-dolerite sill of the Katangsky complex (~400 m thickness) with the Ordovician carbonate-terrigenous rocks of the Proletarsky Formation was studied in the Podkamennaya Tunguska river valley (Figs. 12a–12e). The sedimentary rocks consist of limestones, dolomites, and marls layers forming wavy-layered texture (Figs. 12b–12d). The most important characteristic of this outcrop is the preserved texture of the sedimentary rocks near their contact with gabbro-dolerites. Thus, the magma practically does not influence the surrounding rocks (at least 20 cm below the contact). It is obvious for the small gabbro-dolerite apophyses penetrating the sediments at an angle (Fig. 12c). Perhaps, a very thin altered zone in carbonate rock occurs, but the direct contact is destroyed by weathering, but its thickness does not exceed 2–5 cm.

Chemical analyses of the samples taken from the contact zone (Fig. 12b, Table S8) support the conclusion of the absence of a strong metamorphic alteration of dolomite (sample BKT-11/1) because it keeps 30.17 wt % CO_2. Organogenic limestones occur 1.2 m below the sill (Fig. 12e), with their structure completely preserved.

The compositions of gabbro-dolerites from the bottom of the sill (samples BKT-11/3 and BKT-11/4) do not show any differences from the typical gabbro-dolerites of the Katangsky complex (Krivolutskaya et al., 2020). This fact indicates the absence of assimilation of carbonates by magma in situ.

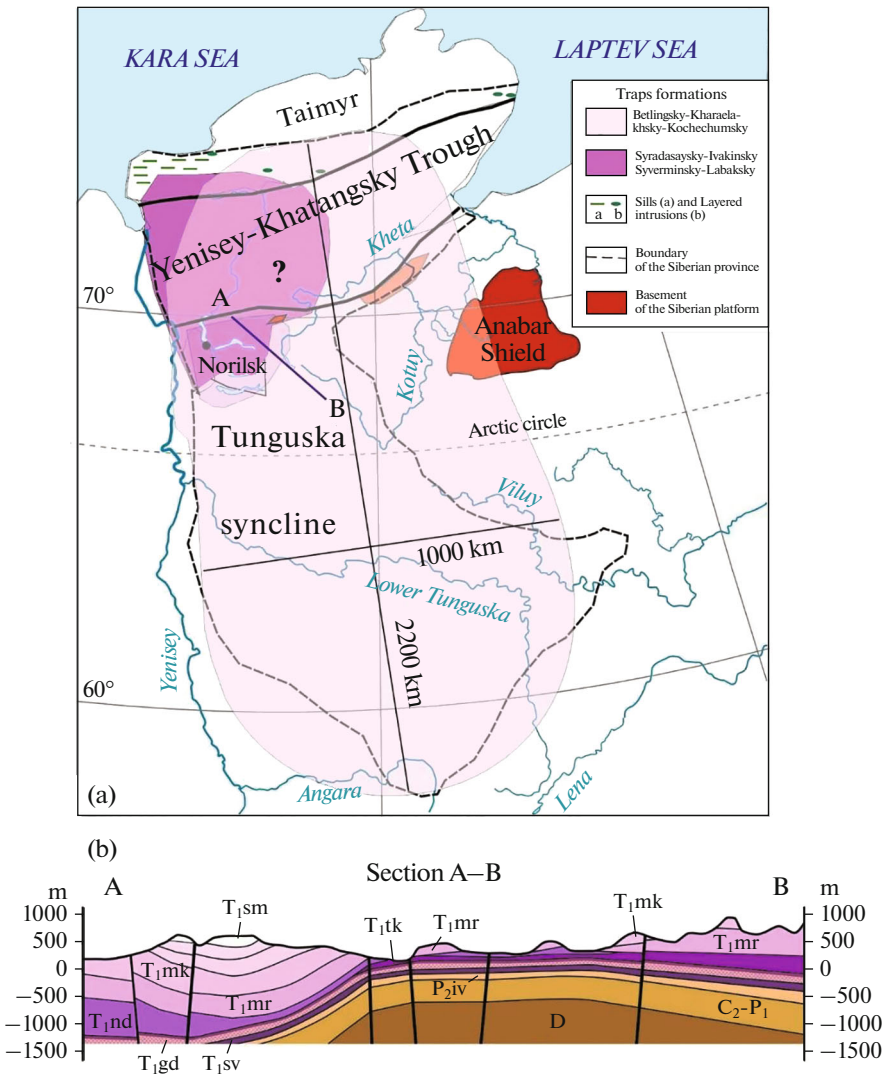

Fig. 11. Schematic geological map of Eastern Siberia (a) and cross-section (b).

As in the contact of the main sill with carbonate rocks, small apophyses, skarns, or other metasomatic rocks are absent in this zone. This geological phenomenon is due to the low H_2O content in the parental trap magma and the low H_2O saturation of sedimentary rocks. It is opposite to the geological phenomenon that occurred during the intrusion of ore-bearing magmas into the water-saturated surrounding rocks in the Norilsk region where metasomatic rocks were formed. Their origin is evidenced by oxygen isotope data showing the participation of meteoritic water (Pokrovsky et al., 2005).

Figure 12f exhibits the second example of the interaction of basalt magma with limestones. The contact of the gabbro-dolerite sill of the Katangsky complex (7 m thick) with the host carbonate rocks is fixed in the Kulyumber river valley. The sill splits into two branches in the carbonate rocks, which do not show essential structural and textural changes near their contact with gabbro-dolerite.

Basalt magma interaction with the coal-bearing rocks. A probable origin of gases that caused the P–T boundary mass extinction is attributed to coal-bearing rocks, widespread within the Tunguska syneclise. Contacts of igneous rocks with coal horizons in Eastern Siberia are quite rare; only basalts that overflowed the rocks of the Tunguska series have a chance to contact with coals. These basalts belong to different formations in different parts of the SLIP, namely, Ivakinsky and Syverminsky in Norilsk, Arydzhansy in Maymecha-Kotuy, and Syradasaysky in Taymyr. These formations' explosive rocks (tuff, tuffit, and tufflava) often contain coal xenoliths. Contacts of intrusive rocks with coal-bearing rocks are more frequent because many gabbro-dolerite sills are located in the Tunguska series. We demonstrate two examples of coal

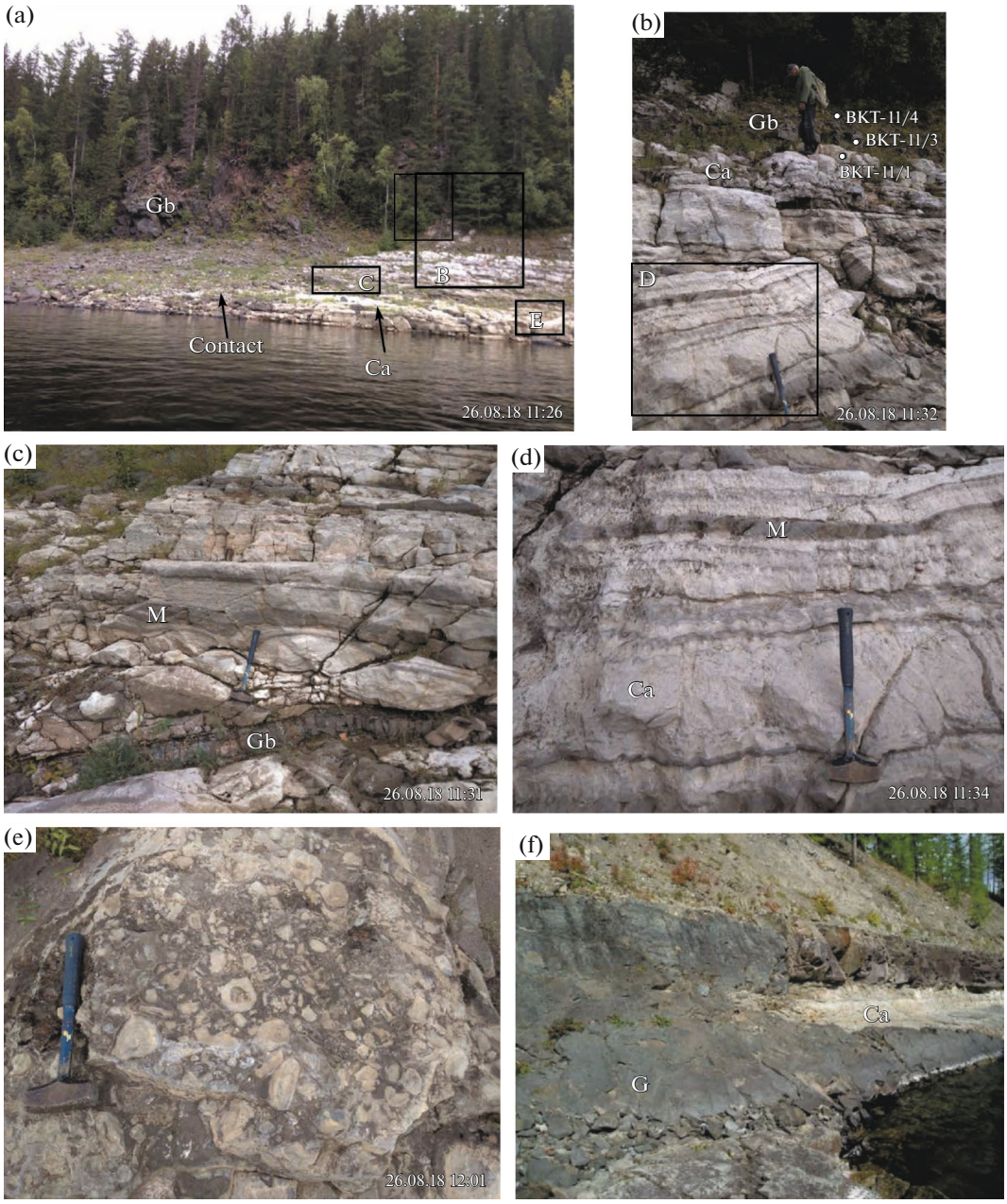

Fig. 12. Contact of the gabbro-dolerite sill (Katangsky intrusive complex) with the Ordovician carbonate-terrigenous rocks (limestones and dolomites, often oolitic and algal), Proletarsky Formation. Podkamennaya Tunguska river valley. (a) General view with photo positions in (b), (c), and (d), (b) contact gabbro-dolerite sill (Gb) with carbonate-terrigenous rocks (Ca). Points are sample locations (number sample corresponds to the number in Table S8), (c) apophysis of gabbro-dolerite sill in carbonate rocks, (d) structure of carbonate-terrigenous rock (a fragment of (b)), (e) contact of gabbro-dolerite sill (Katangsky intrusive complex) with Devonian carbonate rocks (Kulyumber river valley). M—marl, G—gabbro, Gb—gabbro-dolerite, BKT-11/4—sample number.

contacts with basalt magma, more accurately, the coal occurs in magmatic rocks.

A geological phenomenon is observed on the side of the Kayerkan coal open pit (KUR-2), Norilsk region. A coal layer is located within the trachybasalts of the Ivakinsky Formation overlapping the coal-bearing rocks of the Tunguska series (Kayerkansky Formation). It lies between two flows (5–6 m thick), stretching several kilometers. The lower trachybasalt flow lies directly on the coal-bearing sandstones and conglomerates, which MMC Nornickel explores. Probably, magma during the introduction "picked up" a layer of coal that floated on its surface; small fragments of coal were also observed in the upper part of the lower flow. The second magma flow blocked the coal layer from the top; in this way, it occurred among the igneous

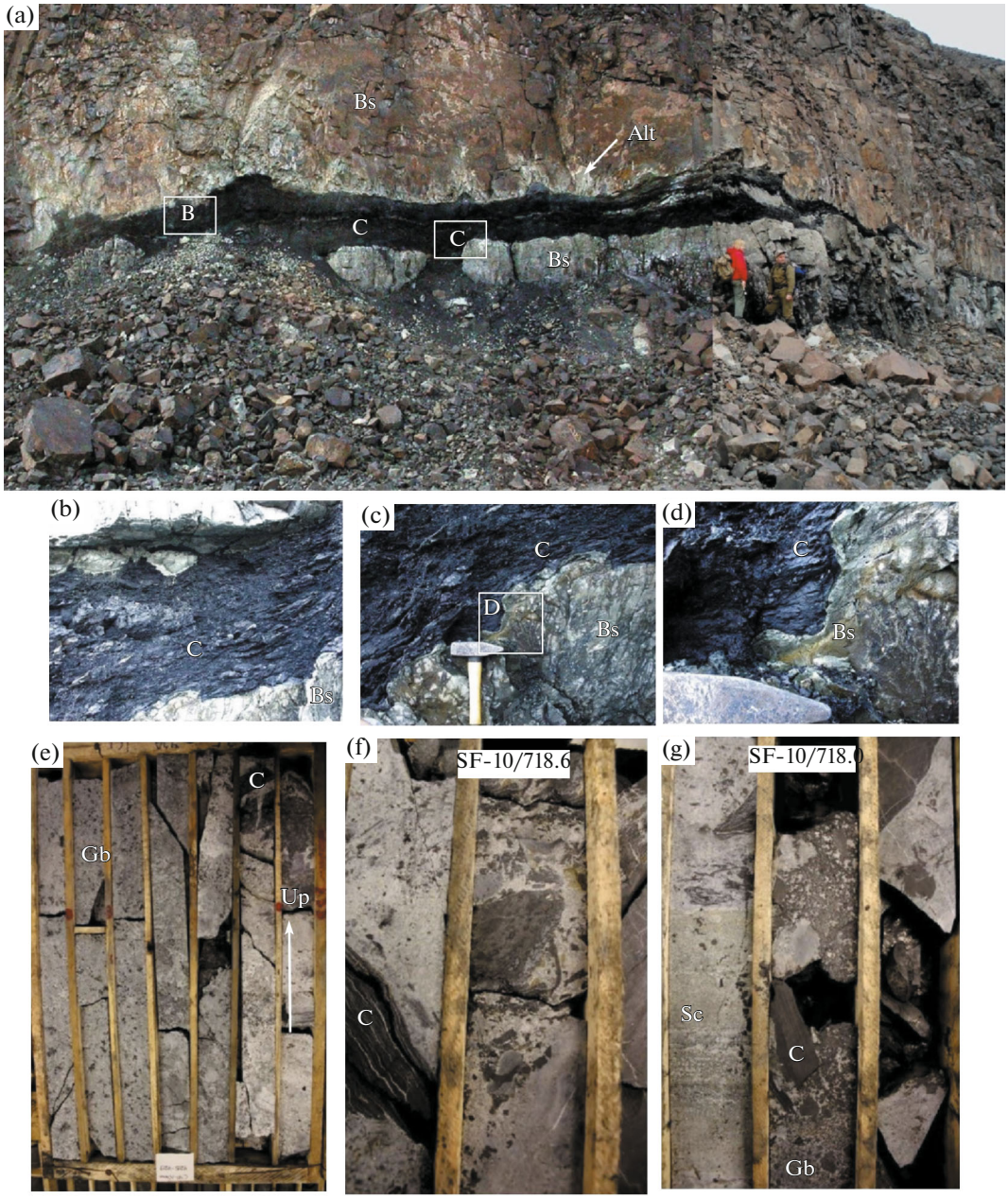

Fig. 13. Contacts of coal with magmatic rocks. (a) Coal layer (c) between two basalts flows (b), Kayerkan open pit, Norilsk area. Alt–zone of alteration in basalts, rectangles show photos demonstrated in (b–d); (b, c) details of (a); (e) detail of (c); (e–g) coal pieces (xenoliths) in the upper zone of the Talnakh intrusion, borehole SF-10, 718 m depth in borehole. Sc–scarn, Gb–gabbro-dolerite. Diameter of core is 4.8 cm.

rocks as xenolith. Despite this position, the structure of coal was not changed by hot magma in its inner part (Fig. 13). Only the 3–4 cm rim of xenolith was impregnated with basalt melt, and volatile components from this coal zone were released, altering the already crystallized magma (trachybasalts). As a result, the 50–60 cm thick light zone (Alt) in basalts was formed under the influence of coal degassing. It is obvious that volatiles could not penetrate the already crystallized magma at a great distance and reach the surface.

The second example of finding coal in igneous rocks can be considered for a sample of the Talnakh intrusion, discovered by the SF-10 borehole. In the upper contact zone of the massif, fragments of coal up to 10 cm in size are installed in leucocratic gabbro-dolerites (Fig. 13e), as well as scarred rocks of this massif. Despite the impact of both magma and fluids that formed scarns on the contact of silicate rocks, coal has not undergone significant changes. A layered texture typical of unchanged coal rocks is observed in its xenoliths.

DISCUSSION

The compositions of initial magmas, including their volatile contents, associated with the Siberian traps have been an important research topic over the past few decades (Zolotukhin et al., 1986; Barnes et al., 2019; Sobolev et al., 2009).

The Fluid Regime and the Origin of the PGE-Cu-Ni Deposits

The fluid regime of basic-ultrabasic magmas has an important role in the origin of PGE-Cu-Ni ores in the Norilsk region. A pioneering work using gas chromatography has shown that H_2 and CH_4 dominated the volatile components in melts, this is evidence of modern gas flow through the faults. Aplonov published this result in 1995. Later, some authors argued that magmas formed ore-bearing intrusions were enriched in H_2O and Cl compared to barren intrusions (Distler et al., 1999; Barnes et al., 2019). Its theoretical basis was unclear because both magmas are intraplate and have similar major and trace element contents. The idea of volatile-rich ore-bearing magma is based on the existence of thick metasomatic halos around the ore-bearing intrusions that were supposed to be formed by magmatic fluids (Turovtsev, 2002). However, according to stable isotope data, not magmatic but meteoric waters took part in the halo formation (Pokrovsky et al., 2005). Bulgakova (1971) was the first researcher who reported data on volatile components in ore-bearing magmas by measuring gases directly in individual inclusions in rock-forming minerals. She showed the predominance of H_2O over CO_2 and the absence of reduced gases in significant quantities. This was later confirmed by Raman spectroscopy and SIMS (Krivolutskaya et al., 2001; Krivolutskaya and Sobolev, 2001). The proximity of H_2O and Cl contents in ore-bearing and barren intrusions was also demonstrated. The results presented above (Table 1, Table S5) confirm the decisive role of these gases in melts.

Traps' Genesis and Volatiles Sources

Siberian traps are the subject of much research on LIP origins. The supposed conditions of magma generations determine sources of volatiles. They are as follows.

The first model suggests that the regime of volatiles depends on plume activity. The first volcanic products of mantle plumes are traps (Campbell and Davies, 2006; Campbell and Griffiths, 1990). Experimental studies in viscous liquids have shown that the "initial" portions should approach the bulbous head in shape, followed by a narrow feeding channel. Hence, rifting begins after the actual trap magmatism, leading to the split of continents (Campbell and Davies, 2006). However, this schema does not apply to the Siberian province, where magmatism begins within rift zones while flood basalts were formed later. Moreover, basalts effusion does not begin with picrites, as it is predicted by the model: only tholeiitic basalts occur in the Tunguska syneclise. Picrites are associated only with the Yenisei-Khatanga rift. For some time, two kinds of magmatism, namely, rift and platform, have operated simultaneously (Krivolutskaya, 2011; Krivolutskaya et al., 2019). Another discrepancy between the real geological situation and this model is the absence of area uplift before traps magmatism. An ascent of a large plume (Siberian "superplume") (Dobretsov, 1997) should lead to an area elevation of 2 km, although it is well known that it was a shallow marine basin (Tesakov, 2014) and a coal continental basin at the end of the Paleozoic epoch. So, there is no proof for the suggested uplift and erosion of the Tunguska rocks based on their stratigraphic nonconformity with basalts. This disagreement does not mean a high altitude of eroded rocks.

To eliminate the uplift problem, it was suggested (Sobolev et al., 2011) the existence of a pyroxenite mantle under the Siberian craton, which is lighter than the peridotite one and, therefore, does not cause a significant elevation. According to this model, volatiles left plume before trap formation. There are some disadvantages to this model. First, it is not consistent the conclusions with the geology of the province. Thus, the Gudchikhinsky picrites regarded as a product of melting of pyroxenite are not the earliest rocks as it is suggested. They overlap the Ivakinsky and Syverminsky basalts characterized by crustal geochemical signatures (Lightfoot et al., 1990). Further, the Gudchikhinsky rocks distribute only in the south shoulder of the Yenisey-Khatanga rift and pinch out to the Tunguska syneclise where flood basalts are located, it is unclear how these rocks link each another. This model does not consider the time and place of subduction that led to pyroxenite formation. Then, it is unclear how replacing the peridotite source with the pyroxenite one influences uplift size because the densities of these rocks are close (from 3 to 3.4 g/cm^3).

Another model was suggested to solve the uplift problem: the model of delamination of Earth's crust, which leads to the melting of the lower and middle crusts because of the collision of two continents (Elkins-Tanton, 2005; Demina et al., 2018). According to our data, this model is more in line with reality, explaining the geochemical features of typical traps (including volatiles components), namely, their crustal characteristics. It supposes delamination due to the collision of the Siberian Craton with the Kara continent at the end of the Paleozoic period. However, significant deformations in Taimyr and the Siberian Craton are post-traps as well (State geological maps S-44–S-46, 1 : 1000000 scale). This inconsistency was not explained.

The third trap model suggests their formation in the subduction zone based on their geochemical character-

istics close to subducted magmas (Ivanov, 2007). In fact, this is only due to an occurrence of crustal material in both magmas, not of the same origin. The low concentrations of volatiles in traps (Tables 1, S5) demonstrate their difference with subduction basalts, where these concentrations are high (Naumov et al., 2017).

An analysis of the deep structure under the trap provinces was performed, and the results showed decreasing *S*-wave velocities at a 460 km depth (Vinnik et al., 2017; Vinnik and Farra, 2007). However, similar signs of a decreasing *S*-wave velocity were also obtained in several regions that do not belong to trap provinces. In the case of delamination beneath the Siberian Craton, stratification of the lithosphere in its lower part due to the intruded hot material should be observed and a decrease in *S*-wave velocities to 4.4–4.5 km/s must be fixed. The absence of such observations means that the question of the mechanism of the Siberian Traps formation needs further study (Vinnik et al., 2017).

Volatiles and Mass Extinction at the P–T Boundary

Estimation of volatiles in trap magmas. A few data on volatile components were previously obtained for typical traps, but the main part of publications is devoted to rift magmas. Sibik with coauthors (2015) investigated inclusions in pyroxenes from the Ayansky and Khonnamakitsky basalts in the Tunguska syneclise and obtained volatile contents lower than the values we obtained in melt inclusions (Table 2). The difference is due to, first, the type of inclusion. The Ayansky and Khonnamakitsky basalts are plagiophyric, that is, they contain only plagioclase as phenocrysts, while pyroxene occurs in the groundmass. Therefore, inclusions in clinopyroxenes reflect the composition of the final stage of magma crystallization, when volatiles have already been largely lost during its degassing on the surface. Second, these results are not representative because the size of inclusions was small (10–20 μm) and was not specified for each inclusion. Unfortunately, there is much confusion in the source data. Hence, samples S10-3–S10-25 are indicated in the text as basalts and S10-29 as sills, while in A in Supplemental A1, the first group is characterized in the description column as "fine-grained dolerite" and the second one as "porphyritic basalt". In addition, the column "Intruded in" for the first group indicates the Tunguska series sediments. It is unclear how the Ayansky and other Triassic basalts of the main magmatic phase could be intruded into lower C_2–P_2 sedimentary rocks if they cover upper *P–T* tuffs and basalts of the Korvunchansky Formation.

Some data were obtained from platform basalts and sills (Black et al., 2012). We do not regard the data from the Arydzhansky Formation because it belongs to rift products. The authors analyzed 3 samples from typical traps: sill from Bratsk (sample A10), sill from Ust-Ilimsk (K06) and basalt of the Onkuchaksky Formation (K09). The most melt inclusions were studied in plagioclase (only 5 inclusions in olivine from 44 inclusions). The size of the inclusions is not indicated. Cl, F, and S were measured. The data are strange because F contents rich up 1.95 wt % and Cl—0.94 wt % in inclusions in plagioclase from gabbrodolerites (sills). At the same time, MgO content is very low in these inclusions, it changes from 0.95 to 3.01. Crystallization of this melt could not give gabbro rocks. Only inclusions in plagioclase from the Onkuchaksky basalts have real element concentrations (wt %): 5.18–7.06 MgO, 0.01 Cl, 0.02–0.16 F, and 0.02–0.04 S, demonstrating real contents of volatiles in magmas. They are close to the Maslovsky intrusion (except fluorine). Despite of sills false compositions, the authors used all these inclusions to determine sulfur isotopes (Black et al., 2014).

Volumes of volatile components are obtained during magma degassing. Effusive rocks are undoubtedly the main source of volatiles. Even subvolcanic rocks do not give fluids that can reach the surface. Thus, their volatiles are mostly kept in magmas, and their contents are maximum compared with the basalts. Therefore, we studied melt inclusions in intrusive rocks. As a second source of volatiles, sedimentary rocks that have undergone heating during interaction with magmas are usually considered. However, the resulting amount of volatiles in this case (Elkins-Tanton et al., 2020; Svensen et al., 2018) is highly overestimated according to our data. Even if small pieces of coal occur in the Ivakinsky basalts, they could not produce much gas volume. In this regard, the arguments given by Davydov (2021) are fair. In a reply (Davydov and Karasev, 2021), they present not geological facts but a theoretical scheme that cannot be proof of a big gas flow. Our data on the coal layer (Fig. 13) show that the gases released from it do not reach the surface.

The occurrence of carbonate rocks between basalt flows demonstrated by Svensen and co-authors (2018) is not a direct evidence of CO_2 production from carbonates. The restricted zone of metamorphism in carbonate-terrigenous rocks and, consequently, the small volume of the possible gas released in this case, is demonstrated in Fig. 12. Furthermore, sills of the Katangsky complex regarded as a source of heat in this interaction correspond to the middle phase of magmatism (to the Mokulaevsky Formation, Latyshev et al., 2013); they intruded after *P–T* boundary and, therefore, their impact on the crisis is unlikely. Similar suggestion of a huge S flow due to the metamorphic reaction of magmas with anhydrite (Sobolev et al., 2009, 2015) is not supported by geological facts and mass-balance calculations. The S degassing of anhydrite due this reaction must led to rock enrichment in CaO which is absent in intrusion exocontacts (Grinenko, 1985; Krivolutskaya et al., 2019a).

The volatile contents in clinopyroxene inclusions (and olivine from the OM-24/666) were taken for cal-

culations because these inclusions provide more reliable information on melts due to their excellent fast homogenization (quenched glasses were obtained) compared with the inclusions in olivines from the picritic gabbro-dolerites (OM-24/814). Furthermore, the compositions of these inclusions are close to typical traps. Therefore, the concentrations of volatiles estimated in the Maslovsky magma are regarded as the maximum possible concentrations in typical trap magmas compared with the basalts degassing on the surface during their crystallization (Table 2). Especially the CO_2 volume realized from basalts should be reduced compared with intrusions ibecause it gets lost very quickly during magma ascent.

Of course, rift magmatism produced some volume of gas as well, but we cannot estimate it because the volume of basalts in Western Siberia is unknown; rare boreholes penetrate basalts here. In general, the volume of volcanic rocks here is much smaller than in Eastern Siberia (it is around 1/5).

Analysis of modern gas fluxes from different types of volcanoes demonstrates their similar volumes. Marty and Tolstikhin (1998) showed that arcs, spreading centers, and plumes may provide a comparable flux of CO_2. The modern summary budget for gas (H_2O, CO_2, S, Cl, F) fluxes from all arc volcanoes was estimated by (Fischer, 2008). In comparison with these data (calculated for 1 My, as a possible time for trap formation) Siberian traps show considerably lower masses of H_2O and CO_2 (11 and 6 times), similar S (or SO_2), yet considerably higher Cl (3 times) and F (20 times) which could be potentially degassed to the Permian-Triassic atmosphere (Table 2). It is unclear which gases and in what quantities have a critical impact on the Earth mass extinction of living species. But it seems that degassing of the Siberian traps was not a catastrophic event compared to the present-day volcanic activity.

The time when these gases were released is also important.

Age and duration of traps magmatism. Despite being well-regarded, there is no reliable evidence for the link between the timings of magmatism and extinction (Bond and Grasby, 2017). To determine the duration of magmatism, the products of its earliest and latest stages must be dated with an accuracy that allows them to be distinguished from each other. So far, this problem has not been solved.

The estimated duration of the formation of traps of less than 1 million has not yet been confirmed. It is based on Kamo data for Norilsk 1 (Kamo et al., 2003) as a reference point for the initial stage of magmatism and perovskite from the maimechites for its final stage. However, the formation of Norilsk 1 corresponds to the Morongovsky-Mokulaevsky formations of the middle stage of magmatism (Godlevsky, 1959; Fedorenko et al., 1996), not initial stage. The duration of 2 million (Latyshev et al., 2020) determined based on the Maimecha-Kotuy section also does not reflect the real length of magmatism because the supposed Late Permian age of the Khardaksky Formation is not indisputable. This formation is geochemically close to the Arydzhangsky Formation, correlated with the Morongovsky-Mokulaevsky formations (Fetisova et al., 2014). It seems very logical and is confirmed by geochemical data (Shtokalo et al., 2021). The rocks of the Arydzhangsky Formation are interlayered with the rocks of the Pravoboyarsky Formation, which is close in composition to the Mokulaevsky basalts.

The data by (Burgess and Bowring, 2015) for zircons and baddeleyites were studied with high precision and did not raise methodological questions. However, their interpretation does not correspond to the geological data. The authors performed the following scheme of magmatism evolution: tuffs–basalts–intrusions. Nevertheless, it is well known that magmatism pulsed in the Siberian Platform (Godlevsky, 1959; Zolotukhin et al., 1986). Not only each formation begins from the tuff horizon, but the tuffs are also regularly present inside them. The most important for evolution is not the tuffs of the Ivakinsky Formation, described by the authors, but the tuffs of the Korvunchansky, Khakanchansky, and Morongovsky Formations (Dyuzhikov et al., 1992; Rudakova and Krivolutskaya, 2009). The attribution of the Norilsk 1 intrusion to the last stage of magmatism also does not correspond to geological data (see above). This scheme (Burgess and Bowring, 2015) is based on the zircon data. Zircons in tuffs cannot be used for dating because they are not crystallized in these rocks. It is almost impossible to separate zircons from basalts. Only intrusive rocks are sources of zircon. In this work (Burgess and Bowring, 2015), zircons were chosen tendentiously: only minerals close to 251.9 Ma. However, it is well known that in intrusive rocks, particularly in Norilsk 1, this mineral has a huge age diversity (Malich et al., 2013; Petrov, 2019). It was demonstrated by both U–Pb and Hf isotope systems (Malich et al., 2013).

According to paleomagnetic data, only the Ivakinsky Formation (and Saradysaysky in Taimyr) was formed in Permian time because their rocks are characterized by reversal magnetization. They occupy less than 1% volume of the whole volcanic rock volume. The basalts of other formations were crystallized in the Triassic period (Masaitis, 1983). The suggestion on the $P–T$ boundary below the Morongovsky Formation (Latyshev et al., 2020, 2020a) does not change the conclusion on the Triassic age of the traps rocks (CFBP).

Problems of mass extinction. In addition to synchronicity with traps, the mass extinction problem has many other aspects. The $P–T$ extinction event has a complex character. The reduction of marine species did not occur simultaneously in the northern and southern latitudes, and its relationship with events on the continents is unclear (Song et al., 2020). Some researchers believe that terrestrial species were reduced

after the marine crisis, while others guessed that it prevented marine extinction. Apparently, these views differ due to objective reasons—the absence of a sharp change in flora and fauna in terrestrial sediments.

These features are also characteristic of the Siberian Platform, where the boundary of Permian and Triassic deposits is not clearly established. In several studies, the same species are considered either Permian or Triassic. It is determined that the flora change is fixed in SW Tunguska syneclise in the basement of the Tutonchansky Formation (tuff, tuffits) were together with ferns *Coradites* and *Pecopteries* were found bivalves *Paleanodonta Biltchanica Mal, P. Linta Ma.l*, that is unknown in underlying deposits but widespread in overlapping rocks (Betekhtina and Mogucheva, 1984). So, all explosive rocks and basalts of the Siberian platform were formed during the Triassic period (Masaitis, 1983). Interesting conclusions were obtained by paleontologists on insects, for which only on the *P–T* boundary a reduction of species was manifested, unlike other similar events. However, Rasnitsyn and co-authors (2015) showed that this reduction was not due to the dominant extinction of species but to the very slow appearance of new species, starting from the middle of Perm. In addition, dragonfly prints were found in the tuffites of the Morongovsky Formation, which indicates the absence of severe conditions during the traps formation. These findings were described in an article with the peculiar title "When life did not even think of dying" (Rasnitsyn, 2012).

The last comment concerns data on the two-step mass extinction at the *P–T* boundary. Song and co-authors (2020) fixed 2 stages of extinction in the Meishan section, i.e., in Perm and Triassic. However, the second event was dated 252.1 Ma. The last decision of the International Commission on Stratigraphy Stratigraphic put the *P–T* boundary at 251.902 ± 0.024 Ma (https://stratigraphy.org/chart). Therefore, the second extinction belongs to the Permian period as well. The multi-stage extinction is not universal and is not fixed for all species. The extinction of the vertebrate fauna at the global level (Sahney and Benton, 2008) occurred due to one stage of extinction at the Permian-Triassic boundary. This is also evidenced by the analysis of terrestrial plants in continental sediments, although Rees (2002) showed that the diversity of plants could change completely differently in different regions.

Answering the question posed in the title of the article, we can say that there is no strict evidence of the influence of traps on the *P–T* extinction of life at the moment.

CONCLUSIONS

(1) The study of the melt inclusions in olivine and clinopyroxene of gabbro-dolerites from the Southern Maslovsky intrusion, which is coeval to the Morongovsky–Mokulaevsky Formations of the Siberian flood basalt province, has shown low contents of volatile contents in its parental melt similar to within-plate magmas.

(2) Relatively low estimated volumes of volatile components released during magma emplacement contradict the statement about the extremely high amount of volatiles accompanying Siberian trap formation. The previous suggestion about volatile enrichment because of the magmas interactions with sedimentary rocks is not supported by the field observation of the contacts of igneous rocks with sedimentary deposits (carbonate-terrigenous and coals rocks), which demonstrates the only narrow zones of alteration between the mentioned layers.

(3) These new data lose the linkage between Siberian trap formation and mass extinction, especially considering that the duration of magmatism on the Siberian platform has not yet been determined. According to geomagnetic data, most magmatic rocks in this region have Triassic age, and the simultaneity of basaltic rock formation with the global biota extinction on the Siberian platform has not yet been proven.

ACKNOWLEDGMENTS

The authors are grateful to Alexander Sobolev for the opportunity to conduct EPMA analyses at the Max Planck Institute of Chemistry in Mainz. We thank Sergey Simakin, Eugeny Potapov for SIMS analyses of melt inclusions and Natalia Kononkova for EPMA analyses of minerals. We express gratitude to Eugeny Karasev for the useful comments.

FUNDING

The research was carried out with the financial support of the Russian Science Foundation (project no. 22-27-00387, analytical work), State Assignment "Processes controlling the formation and evolution of the Earth's lithosphere" 0137-2019-0012 (field trip), and no. 121041500233-0 (petrographical study of the Maslovsky gabbro-dolerite intrusion).

CONFLICT OF INTEREST

The authors declare that they have no conflicts of interest.

SUPPLEMENTARY INFORMATION

The online version contains supplementary material available at https://doi.org/10.1134/S0016702922130067.

REFERENCES

A. I. Al'mukhamedov, A. Y. Medvedev, and V. V. Zolotukhin, "Evolutions of Permo–Triassic basalts of the Siberian Platform in time and space," Petrology **12**, 339–353 (2004).

V. S. Aplonov, "Fluid regime and platinum potential problems of basic differentiated intrusions," *Platinum of*

Russia (Geoinformmark, Moscow, 1995), pp. 102–106 [in Russian].

N. Arndt, K. Lehnert, and Y. Vasil'ev, "Meimechites: highly magnesian lithosphere-contaminated alkaline magmas from deep subcontinental mantle," Lithos **34**, 41–59 (1995).

N. T. Arndt, G. K. Czamamanske, R. J. Walker, C. Chauvel, and V. A. Fedorenko, "Geochemistry and origin of the intrusive hosts of the Noril'sk–Talnakh Cu–Ni–PGE sulfide deposits," Econ. Geol. **98**, 495–515 (2003).

S.-J. Barnes, Vaillant M. Le, B. Godel, and M. Lesher, "Droplets and bubbles: Solidification of sulfide-rich vapor-saturated orthocumulates in the Norilsk–Talnakh Ni–Cu–PGE intrusions," J. Petrol. **60**, 269–300 (2019).

O. A. Betekhtina and N. K. Mogucheva, "On the age of volcanogenic pile of the Tunguska syneclise," In Stratigraphy, Triassic flora and fauna in Siberia (Tr. Inst. Geol. Geofiz., 1984), pp. 4–8 [in Russian].

B. A. Black, L. T. Elkins-Tanton, M. C. Rowe, and I. U. Peate, "Magnitude and consequence and volatile realized from the Siberian traps," Earth Planet. Sci. Lett. **317–318**, 363–373 (2012).

B. A. Black, H. E. H. Auri, L. T. Elkins-Tanton, and S. M. Brown, "Sulfur isotopic evidence for sources of volatiles in Siberian Traps magmas," Earth Planet. Sci. Lett. **394**, 58–69 (2014).

D. P.G. Bond and S. E. Grasby, "On the causes of mass extinctions," Paleogeogr., Paleoclimatol., Paleoecol. **487**, 3–29 (2017).

E. N. Bulgakova, "Physics–chemical conditions of formation of the Norilsk traps intrusions," In *Traps of the Siberian Platform and Their Metallogeny*, (Irkutsk, 1971), pp. 36–37 [in Russian].

S. D. Burgess and S. A. Bowring, "High–precision geochronology confirms voluminous magmatism before, during, and after Earth's most severe extinction," Sci. Adv. **1**, e1500470 (2015).

I. H. Campbell and G. F. Davies, "Do mantle plumes exist?" Episodes **29** (3), 162–168 (2006).

I. H. Campbell and R. W. Griffiths, "Implications of mantle plume structure for the evolution of flood basalts," Earth Planet Sci. Lett. **99** (1–2), 79–93 (1990).

I. H. Campbell, G. K. Czamanske, V. A. Fedorenko, R. I. Hill, and V. K. Stepanov, "Synchronism of the Siberian Traps and the Permian–Triassic boundary," Science **258**, 1760–1763 (1992).

L. V. Danyushevsky and P. Plechov, "Petrolog3: Integrated software for modeling crystallization processes," Geochem., Geophys., Geosyst. **12**, Q07021 (2011).

V. I. Davydov, "Tunguska coals, Siberian sills and the Permian-Triassic extinction," Earth–Sci. Rev. **212**, 103438 (2021).

V. I. Davydov and E. V. Karasev, "The Influence of the Permian–Triassic magmatism in the Tunguska Basin, Siberia on the regional floristic biota of the Permian–Triassic transition in the region," Front. Earth Sci. **9**, 635179 (2021). https://doi.org/10.3389/feart.2021.635179

V. I. Davydov, E. V. Karasev, and V. V. Zharinova, "Field evidence for coal combustion links the 252 Ma Siberian traps with global carbon disruption," Comment: Geology **49**, e517 (2021).

L. I. Demina, V. S. Zakharov, M. Yu. Promyslova, and S. P. Zaviyalov, "Relations of collision and trap magmatism in Taimyr on the basis of geological data and modeling," Moscow Univ. Bull. **4** (1), 16–25 (2018).

V. V. Distler, S. F. Sluzhenikin, L. J. Cabri, N. A. Krivolutskaya, D. M. Turovtsev, T. A. Golovanova, A. V. Mokhov, V. V. Knauf, and O. I. Oleshkevich, "Platinum ores of the Noril'sk Layered intrusions: magmatic and fluid concentration of noble metals," Geol. Ore Deposits **41** (3), 214–237 (1999).

N. L. Dobretsov, "Mantle superplumes as a reason of main geological periodicity and global reconstructions," Dokl. Earth Sci. **357** (6), 797–800 (1997).

O. A. Dyuzhikov, V. V. Distler, B. M. Strunin, A. K. Mkrtychyan, M. L. Sherman, S. F. Sluzhenikin, and A. M. Lurye, *Geology and Metallogeny of Sulfide Deposits, Noril'sk Region, USSR* (Economic Geology Publishing Company, Littleton, 1992).

L. T. Elkins–Tanton, "Continental magmatism caused by lithospheric delamination," In *Plates, Plumes and Paradigms,* Ed. by G. R. Foulger, J. H. Natland, D. C. Presnall, and D. L. Anderson (Geological Society of America, Boulder, 2005), pp. 449–461.

L. T. Elkins-Tanton, S. E. Grasby, B. A. Black, R. V. Veselovskiy, O. H. Ardakani, and F. Goodarzi, "Field evidence for coal combustion links the 252 Ma Siberian traps with global carbon disruption," Geology **48**, 986–991 (2020).

L. T. Elkins-Tanton, S. E. Grasby, B. A. Black, R. V. Veselovskiy, O. H. Ardakani, and F. Goodarzi, "Field evidence for coal combustion links the 252 Ma Siberian traps with global carbon disruption: Reply," Geology **49** (3), e518–e518 (2021).

R. Ernst, *Large Igneous Provinces* (Cambridge University Press, 2014).

V. Fedorenko and G. Czamanske, "Results of new field and geochemical studies of the volcanic and intrusive rocks of the Maymecha–Kotuy area, Siberian flood-basalt province, Russia," Int. Geol. Rev. **39**, 479–531 (1997).

V. A. Fedorenko, P. C. Lightfoot, and A. J. Naldrett, "Petrogenesis of the Siberian flood-basalts sequence at Noril'sk, north–central Siberia," Int. Geol. Rev. **38**, 99–135 (1996).

A. M. Fetisova, R. V. Veselovskiy, A. V. Latyshev, V. A. Rad'ko, and V. E. Pavlov, "Magnetic Stratigraphy of the Permian–Triassic traps in the Kotuy River Valley (Siberian Platform). New paleomagnetic data," Stratigraphy. Geol. Correlation **22**, 377–390 (2014).

T. P. Fischer, "Fluxes of volatiles (H_2O, CO_2, N_2, Cl, F) from arc volcanoes," Geochem. J. **42**, 21–38 (2008).

C. E. Ford, D. G. Russel, J. A. Graven, et al., "Olivine–liquid equilibria: temperature, pressure and composition dependence of the crystal. Liquid cation partition coefficients for Mg, Fe^{2+}, Ca and Mn," J. Petrol. **24**, 256–265 (1983).

Geological Dictionary (VSEGEI, St. Petersburg, 2009) [in Russian].

Geological Map of the Deposits of the Krasnoyarsk District, Tyva Republics, and Khakasia on a Scale 1 : 1500000

Ed. by M. B. Kalvitsky (Krasnoyarsk, 2005) [in Russian].

M. N. Godlevsky, *Traps and Ore-bearing Intrusions in the Norilsk area* (Gosgeoltekhizdat, Moscow, 1959) [in Russian].

L. N. Grinenko, "Sources of sulfur of the nickeliferous and barren gabbrodolerite intrusions of the northwest Siberian platform," Int. Geol. Rev. **27**, 695–708 (1985).

D. R. Haughton, P. L. Roeder, and J. B. Skinner, "Solubility of sulfur in mafic magmas," Econ. Geol. **69** (4), 451–467 (1974).

A. V. Ivanov, "Evaluation of different models for the origin of the Siberian traps," In: *Plate, Plumes, and Planetary Processes,* Spec. Pap. - Geol. Soc. Am. **430**, 669–691 (2007).

S. L. Kamo, G. K. Czamanske, and Y. Amelin, "Rapid eruption of Siberian flood-volcanic rocks and evidence for coincidence with the Permian–Triassic boundary and mass extinction at 251 Ma," Earth Planet. Sci. Lett. **214**, 75–91 (2003).

V. K. Karandashev, V. A. Khvostikov, S. V. Nosenko, and Z. Burmii, "Stable highly enriched isotopes in routine analyses of rocks, soils, grounds, and sediments by ICP–MS," Inorg. Mater. **53**, 1432–1441 (2017).

A. K. Kargal'tsev, M. V. Volovetskii, A. A. Kadik, and O. A. Lukanin, "A high-temperature furnace with a controlled oxygen regime for studying phase and redox reactions in silicate and oxide systems at 1 atm," Geochem. Int. **47** (7), 725–730 (2009).

A. M. Koleszar, A. E. Saal, and E. H. Hauri, "The volatiles contents of the Galapagos plume: evidence for H_2O and F open system behavior in melt inclusions," Earth Planet. Sci. Lett. **287**, 442–452 (2009).

N. A. Krivolutskaya, "The problem of subdivision of volcanic rocks of the trappean formation of the Norilsk region," Dokl. Earth Sci. **439** (2), 1088–1092 (2011).

N. A. Krivolutskaya, *Siberian Traps and Pt–Cu–Ni Deposits in the Noril'sk Area* (Springer, Heidelberg, 2016).

N. A. Krivolutskaya and A. V. Sobolev, "Magmatic inclusions in olivines from intrusions of the Noril'sk region, Northwestern Siberian platform: evidence for primary melts," Dokl. Earth Sci. **381** (3), 1047–1052 (2001).

N. A. Krivolutskaya and T. B. Kedrovskaya, "Structure and composition of the nadayansky lava flow: an example of the homogeneity of lava flows of the Siberian Traps Province," Geochem. Int. **58** (4), 363–376 (2020).

N. A. Krivolutskaya, A. V. Sobolev, S. F. Sluzhenikin, and N. M. Svirskaya, "Melt inclusions in olivines of the Talnakh type intrusions," In *Proceedings of the X International Conference on the Thermobarogeochemistry* (VNII-SIMS, Aleksandrov, 2001), pp. 141–157 [in Russian].

N. A. Krivolutskaya, A. V. Sobolev, S. G. Snisar, B. I. Gongalskiy, B. Hauff, D. V. Kuzmin, I. N. Tushentsova, N. M. Svirskaya, N. N. Kononkova, and T. B. Schlychkova, "Mineralogy, geochemistry and stratigraphy of the Maslovsky Pt–Cu–Ni sulfide deposit, Noril'sk Region, Russia: Implications for relationship of ore–bearing intrusions and lavas," Mineral. Deposit **47**, 69–88 (2012a).

N. A. Krivolutskaya, A. V. Sobolev, V. N. Mikhailov, A. A. Plechova, Yu. A. Kostitsyn, I. A. Roschina, and Z. Fekiacova, "Parental melt of the Nadezhdinsky Formation: geochemistry, petrology and connection with Cu–Ni deposits (Noril'sk area, Russia)," Chem. Geol. **302–303**, 87–105 (2012b).

N. A. Krivolutskaya, A. Latyshev, A. Dolgal, B. Gongalsky, E. Makareva, A. Makarev, N. Svirskaya, Ya. Bychkova, A. Yakushev, and A. Asavin, "Unique PGE–Cu–Ni Noril'sk deposits, Siberian Trap Province: magmatic and tectonic factors in their origin," Minerals **9** (1), 66 (2019a).

N. Krivolutskaya, B. Gongalsky, T. Kedrovskaya, I. Kubrakova, O. Tyutyunnik, V. Chikatueva, Y. Bychkova, E. Kovalchuk, A. Yakushev, and N. Kononkova, "Geology of the western flanks of the Oktyabr'skoe Deposit, Noril'sk District, Russia: evidence of a closed magmatic system," Mineral. Deposit. **54**, 611–630 (2019b).

N. Krivolutskaya, B. Belyatsky, B. Gongalsky, A. Dolgal, A. Lapkovsky, and T. Bayanova, "Petrographical and geochemical characteristics of magmatic rocks in the Northwestern Siberian Traps Province, Kulyumber River Valley. Part II: Rocks of the Kulyumber Sites," Minerals **10**, 409 (2020).

A. V. Latyshev, R. V. Veselovskiy, A. V. Ivanov, A. M. Fetisova, and V. E. Pavlov, "Short intense bursts in magmatic activity in the south of Siberian Platform (Angara Taseeva Depression): the paleomagnetic evidence," Izv. Phys. Solid Earth **49**, 823–835 (2013).

A. V. Latyshev, V. A. Rad'ko, R. V. Veselovskiy, A. M. Fetisova, and V. E. Pavlov, "Correlation of the Permian–Triassic ore-bearing intrusions of the Norilsk Region with the volcanic sequence of the Siberian Traps based on paleomagnetic data," Econ. Geol. **115** (6), 1173–1193 (2020a).

A. V. Latyshev, A. M. Fetisova, and R. V. Veselovskiy, "Linking Siberian Traps LIP emplacement and end Permian mass extinction: evidence from magnetic stratigraphy of the Maymecha–Kotuy volcanic section," Geosciences **10**, 295 (2020b).

P. S. Lightfoot, A. J. Naldrett, and N. S. Gorbachev, "Geochemistry of the Siberian trap of the Noril'sk area, USSR, with amplication for the relative contributions of crust and mantle to flood basalt magmatism," Contrib Mineral Petrol. **104**, 631–644 (1990).

P. C. Lightfoot, C. J. Hawkesworth, J. Hergt, A. J. Naldrett, N. S. Gorbachev, and V. A. Fedorenko, "Remobilisation of the continental lithosphere by a mantle plume: major-, trace-element, and Sr-, Nd-, and Pb–isotopic evidence from picritic and tholeiitic lavas of the Noril'sk District, Siberian Trap, Russia," Contrib Mineral Petrol. **114**, 171–188 (1993).

A. P. Likhachev, "The role of leucocratic gabbro in the origin of Noril'sk differentiated intrusions," Izv. Akad. Nauk SSSR Ser. Geol. **12**, 50–66 (in Russian) (1965).

A. P. Likhachev, *Platinum–Copper–Nickel and Platinum Deposits* (Eslan, Moscow, 2006) [in Russian].

A. P. Likhachev, "Possibility of mantle magma self-enrichment in ore matter and heavy isotope ^{34}S to form platinum-copper-nickel deposits. Perspectives of ore localization in the Norilsk region," Otechestvennaya Geol., No. 3, 32–49 (2019). (In Russian)

K. N. Malitch, E. A. Belousova, W. L. Griffin, and I. Yu. Badanina, "Hafnium-neodymium constraints on sources heterogeneity of the economic ultramafic-maf-

ic Noril'sk-1 intrusion (Russia)," Lithos **164–167**, 36–46 (2013).

B. Marty and I. N. Tolstikhin, "CO_2 fluxes from mid–ocean ridges, arcs and plumes," Chem. Geol. **145**, 233–248 (1998).

V. L. Masaitis, "Permian and Triassic volcanism of Siberia: problems of dynamic reconstructions," Zap Vsesoyuz. Mineral. O-va **112**, 412–425 (1983).

A. J. Naldrett, *Magmatic Sulfide Deposits: Geology, Geochemistry and Exploration* (Springer, Heidelberg, 2004).

V. B. Naumov, V. A. Dorofeeva, A. V. Girnis, and V. V. Yarmolyuk, "Mean contents of volatile components, major and trace elements in magmatic melts in major geodynamic environments on Earth. I. Mafic melts," Geochem. Int. **55**, 629–653 (2017).

G. V. Nesterenko and A. I. Al'mukhamedov, *Geochemistry of Differentiated Traps* (Nauka, Moscow, 1973) [in Russian].

A. A. Nosova, L. V. Sazonova, V. V. Narkisova, and S. G. Simakin, "Minor elements in clinopyroxene from Paleozoic volcanics of the Tagil island arc in the Central Urals," Geochem. Int. **40** (3), 219–232 (2002).

O. V. Petrov, *Isotope Geology of the Norilsk Deposits* (Springer, Berlin/Heidelberg, 2019).

B. G. Pokrovsky, S. F. Sluzhenikin, and N. A. Krivolutskaya, "Interaction conditions of Noril'sk trap intrusions with their host rocks: isotopic (O,H, and C) evidence," Petrology **13** (1), 49–72 (2005).

Proceedings of the Sudbury–Noril'sk Symposium, Ed. by P. C. Lightfoot and A. J.Naldrett (Ontario Geological Survey, 1994).

K. Putirka, "Excess temperatures at ocean islands: Implications for mantle layering and convection," Geology **36** (4), 283–286 (2008).

V. A. Radko, *Facies of Intrusive and Effusive Magmatism in the Norilsk Region* (VSEGEI: St. Petersburg, 2016). [in Russian].

A. P. Rasnitsyn, "When life did not even think of dying," Russian Nature **12**, 39–48 (2012).

A. P. Rasnitsyn, D. S. Aristov, and D. A. Rasnitsyn, "Dynamics of insect diversity during the Early and Middle Permian," Paleontol. J. **49** (12), 1282–1309 (2015).

P. M. Rees, "Land-plant diversity and the end–Permian mass extinction. Geology **30** (9), 827–830 (2002).

M. K. Reichow, M. S. Pringle, A. I. Al'Mukhamedov et al., "The timing and extent of the eruption of the Siberian traps large igneous province: implications for the end-Permian environmental crisis," Earth Planet. Sci. Lett. **277**, 9–20 (2009).

P. R. Renne and A. R. Basu, "Rapid eruption of the Siberian Traps flood basalts at the Permo–Triassic boundary," Science **253**, 176–179 (1991).

A. V. Rudakova and N. A. Krivolutskaya, "Structural and textural specific features of rocks of trap rock association in the Noril'sk trough (NW of Siberian Platform)," Moscow Univ. Geol. Bull. **64**, 364–370 (2009)

I. D. Ryabchikov, I. P. Solovova, T. Ntaflos, A. Büchl, and P. I. Tikhonenkov, "Subalkaline picrobasalts and plateau basalts from Putorana plateau (Siberian CFB province). II. Melt intrusion chemistry, composition of "primary" magmas and P–T regime at the base of superplume," Geochem. Int. **39**, 484–497 (2001a).

I. D. Ryabchikov, T. Ntaflos, A. Büchl, and I. P. Solovova, "Subalkaline picrobasalts and plateau basalts from Putorana plateau (Siberian CFB province). I. Mineral compositions and geochemistry of major and trace elements," Geochem. Int. **39**, 467–483 (2001b).

I. D. Ryabchikov, L. N. Kogarko, and I. P. Solovova, "Physico-chemical conditions of magma formation at the base of the Siberian Plume: insight from the investigation of melt inclusions in the meymechites and alkali picrites of the Maimecha–Kotui Province," Petrology **17** (3), 287–299 (2009).

A. E. Saal, E. H. Hauri, C. H. Langmuir, and M. R. Perfit, "Vapour undersaturation in primitive mid-ocean-ridge basalt and the volatile content of Earth's upper mantle," Nature **419** (6906), 451–455 (2002).

S. Sahney and M. J. Benton, "Recovery from the most profound mass extinction of all time," Proc. Biol. Sci. **275** (1636), 759–765 (2008).

A. Saunders and M. Reichow, "The Siberian Traps and the end-Permian mass extinction: a critical review," Chin. Sci. Bull. **54** (1), 20–37 (2009).

M. Sharma, "Siberian traps," In *Large Igneous Provinces: Continental, Oceanic, and Planetary Flood Volcanism,* Ed. by J. J. Mahoney and M. F. Coffin, Geophys. Monograph Ser. **100**, 273–295 (1997).

R. V. Shtokalo, N. A. Krivolutskaya, A. A. Konyshev, I. T. Rass, and S. I. Demidova, "Composition, structure and formation conditions of the Arydzhangsky Formation of the Maimecha–Kotuy District of the Siberian Trap Province," IOP Conference Series Earth and Environmental Science **962** (1), 012059 (2021).

S. Sibik, M. Edmonds, J. Maclennan, and H. Svensen, "Magmas erupted during the main pulse of Siberian Traps volcanism were volatile-poor," J. Petrol. **56** (11), 2089–2116 (2015).

S. Sibik, M. Edmonds, B. Villemant, H. H. Svensen, A. G. Polozov, and S. Planke, "Halogen enrichment of Siberian Traps magmas during interaction with evaporites," Front. Earth Sci. **9**, 741447 (2021). https://doi.org/10.3389/feart.2021.741447

A. V. Sobolev, "Melt inclusions in minerals as a source of principal petrologic information," Petrology **4**, 209-220 (1996).

A. V. Sobolev and A. B. Slutsky, "Composition and crystallization conditions of the parental melt of the Siberian meymechites in connection with the general problem of ultrabasic magmas," Geol. Geophys. **12**, 97–110 (1984).

A. V. Sobolev, S. V. Sobolev, D. V. Kuzmin, K. N. Petrunin, and A.G. Malitch, "Siberian meimechites: Origin and relation to flood basalts and kimberlites," Rus. Geol. Geophys. **50**, 999–1033 (2009a).

A. V. Sobolev, N. A. Krivolutskaya, and D. V. Kuzmin, "Petrology of primary melts and mantle sources of the Siberian traps province," Petrology **17**, 276–310 (2009b).

S. V. Sobolev, A. V. Sobolev, D. V. Kuzmin, N. A. Krivolutskaya, A. G. Petrunin, N. T. Arndt, V. A. Rad'ko, and Yu. R. Vasil'ev, "Linking mantle plumes, large igneous provinces and environmental catastrophes," Nature **477**, 312–316 (2011).

A. V. Sobolev, N. Arndt, N. A. Krivolutskaya, D. V. Kuzmin, and S. V. Sobolev, "The origin of gases that caused the Permian–Triassic extinction," In *Volcanism and Global Environmental Change*, Ed. by A. Schmidt, K. E. Fristad, and L. T. Elkins-Tanton (Cambridge University Press, Cambridge, 2015), pp. 147–163.

H. Song, S. Huang, E. Jia, X. Dai, P. B. Wignall, and A. M. Dunhill, "Flat latitudinal diversity gradient caused by the Permian–Triassic mass extinction," Proc. Natl. Acad. Sci. U. S. A. **117**, 17578–17583 (2020).

V. S. Staroseltsev, *Tectonics of Lava Plateaus* (Nedra, Moscow, 1989) [in Russian].

H. H. Svensen, S. Frolov, G. G. Akhmanov, A. G. Polozov, D. A. Jerram, O. V. Shiganova, N. V. Melnikov, K. Iyer, and S. Planke, "Sills and gas generation in the Siberian Traps," Philos. Trans. R. Soc., A. (2018) https://doi.org/10.1098/rsta.2017.0080

T. V. Svetlitskaya and P. A. Nevolko, "Late Permian-Early Triassic traps of the Kuznetsk Basin, Russia: geochemistry and petrogenesis in respect to the extension of the Siberian Large Igneous Province," Gondwana Res. **39**, 57–76 (2016).

Y. I. Tesakov, *The Silurian Basin of Eastern Siberia: Basin Paleogeography (on a Chronosonal and Biogeocenotic Basis)* (INGG, Novosibirsk, 2014) [in Russian].

D. M. Turovtsev, *Contact Metamorphism of the Norilsk Intrusions* (Nauchny mir, Moscow, 2002) [in Russian].

N. N. Urvantsev, "North Siberian Ni-bearing province," Rus. Geol. Geophys. **3**, 3–11 (1974).

Yu. R. Vasil'ev, M. P. Gora, and D. V. Kuz'min, "Petrology of foidiitic and meymechitic volcanism in the Maimecha–Kotui province," Russ. Geol. Geophys. **58** (6), 817–833 (2017).

L. Vinnik and V. Farra, "Low S velocity atop the 410-km discontinuity and mantle plumes," Earth Planet. Sci. Lett. **262** (3), 398–412 (2007).

L. P. Vinnik, S. I. Oreshin, and L. I. Makeyeva, "Siberian traps: hypotheses and seismology data," Izv., Phys. Solid Earth **53** (3), 332–340 (2017).

J. L. Wooden, G. K. Czamanske, V. A. Fedorenko, N. T. Arndt, C. Chauvel, R. M. Bouse, B. S. King, R. J. Knight, and D. F. Siems, "Isotopic and trace-element constraints on mantle and crustal contributions to Siberian continental flood basalts, Norilsk area, Siberia," Geochim. Cosmochim. Acta **57**, 3677–3704 (1993).

Z. Yao and J. Mungall, "Linking the Siberian flood basalts and giant PGE-Cu–Ni sulfide deposits at Norilsk," J. Geophys. Res.: Solid Earth **126**, JBO20823 (2020).

V. V. Zolotukhin, V. V. Ryabov, Y. R. Vasil'ev, and B. A. Shatkov, *Petrology of the Talnakh Differentiated Ore–Bearing Trap Intrusion* (Nauka, Novosibirsk, 1975) [In Russian].

V. V. Zolotukhin, O. A. Dyuzhikov, and A. M. Vilensky, *Basalts of the Siberian Platform* (Nauka, Novosibirsk, 1986). [in Russian].

V. V. Zolotukhin, Y. R. Vasil'ev, and O. A. Dyuzhikov, *Diversity of Traps and Initial Magmas: a Case of the Siberian Platform* (Nauka, Novosibirsk, 1989) [in Russian].